

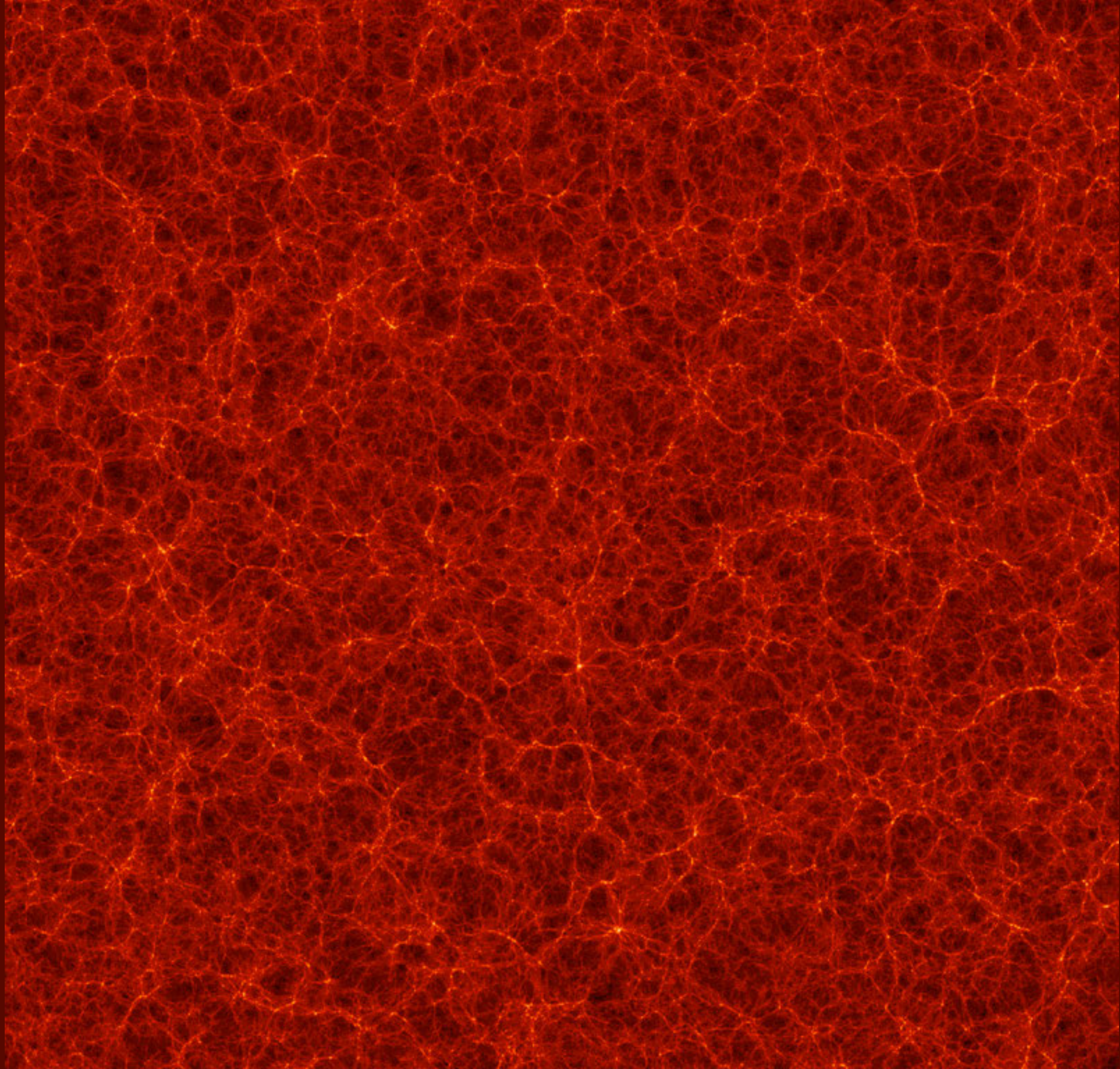
Nonlinear evolution-I: Large-Scale structure

Filaments, voids and clusters.
Power spectra and correlation functions.

$z=0.53$

1 Gpc

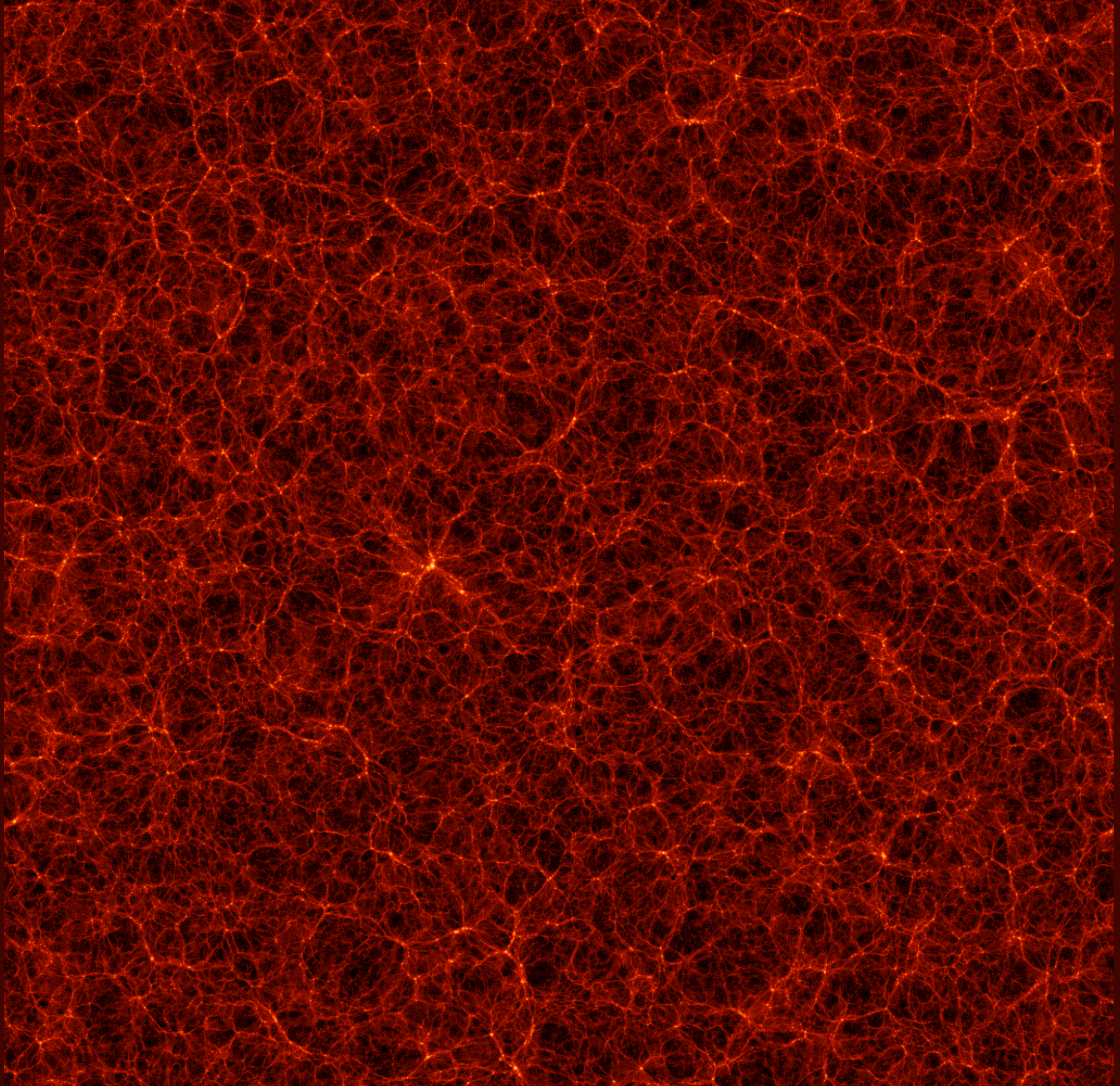
10Mpc slice



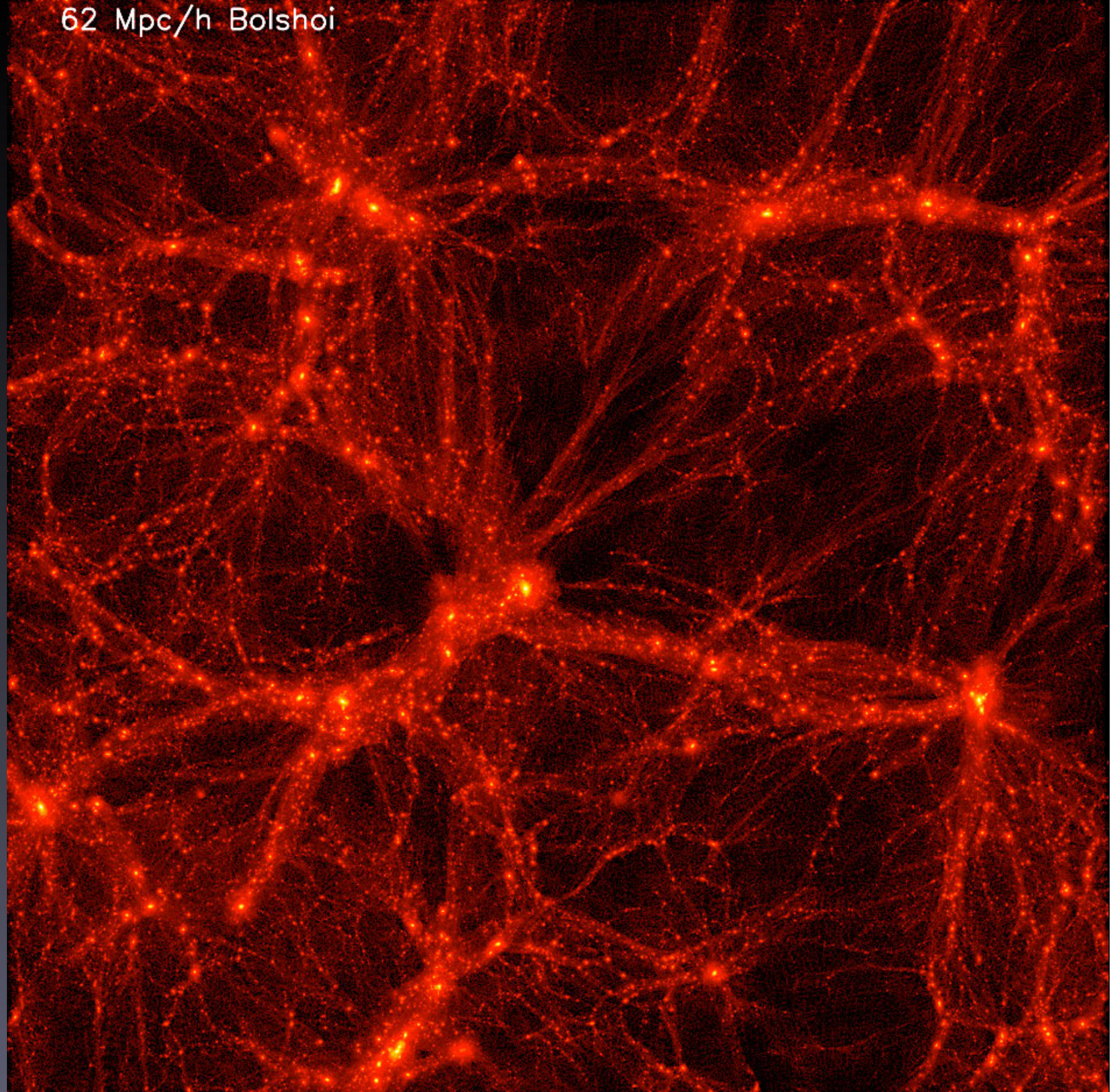
$z = 0$

1 Gpc

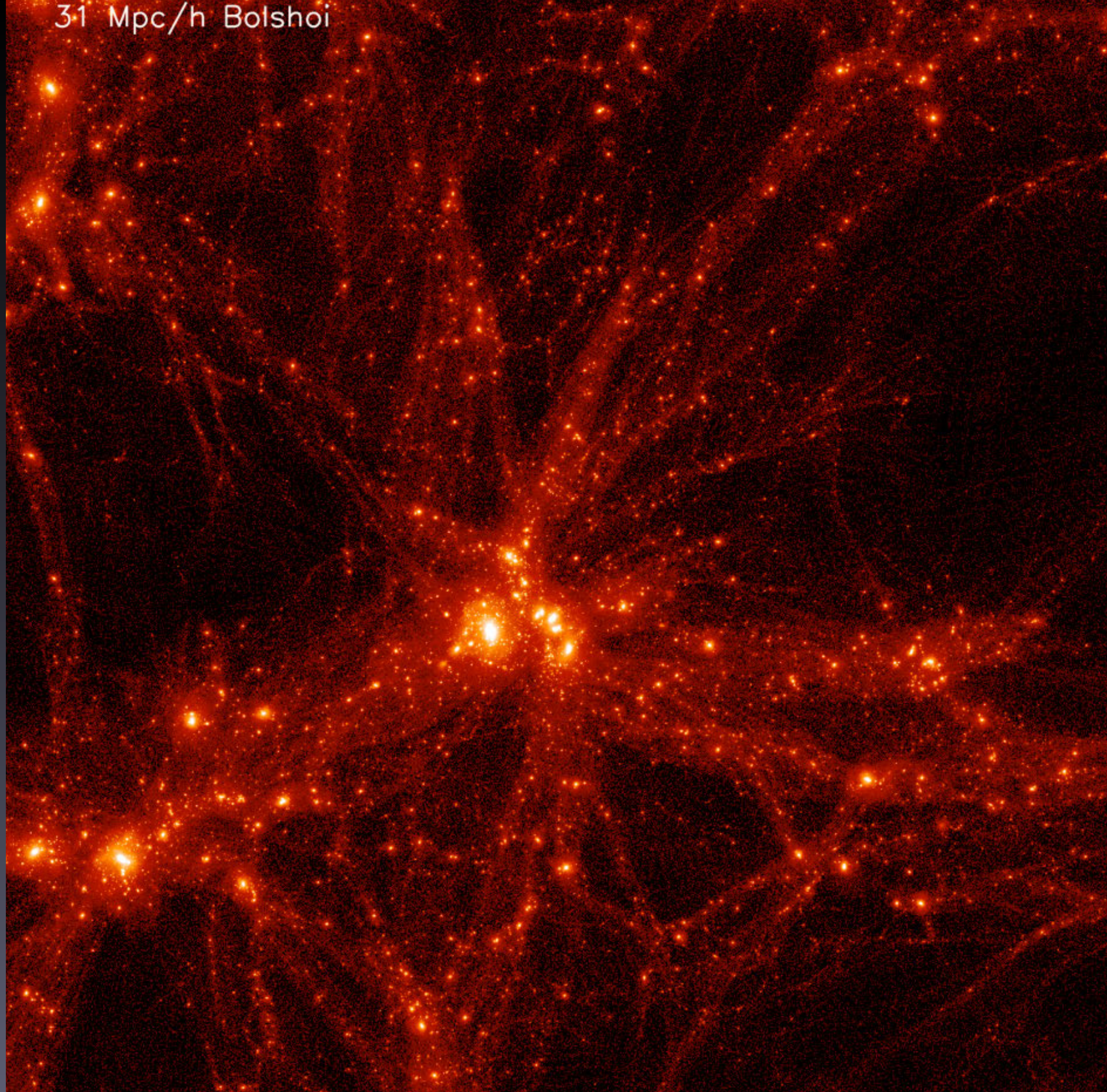
5Mpc slice

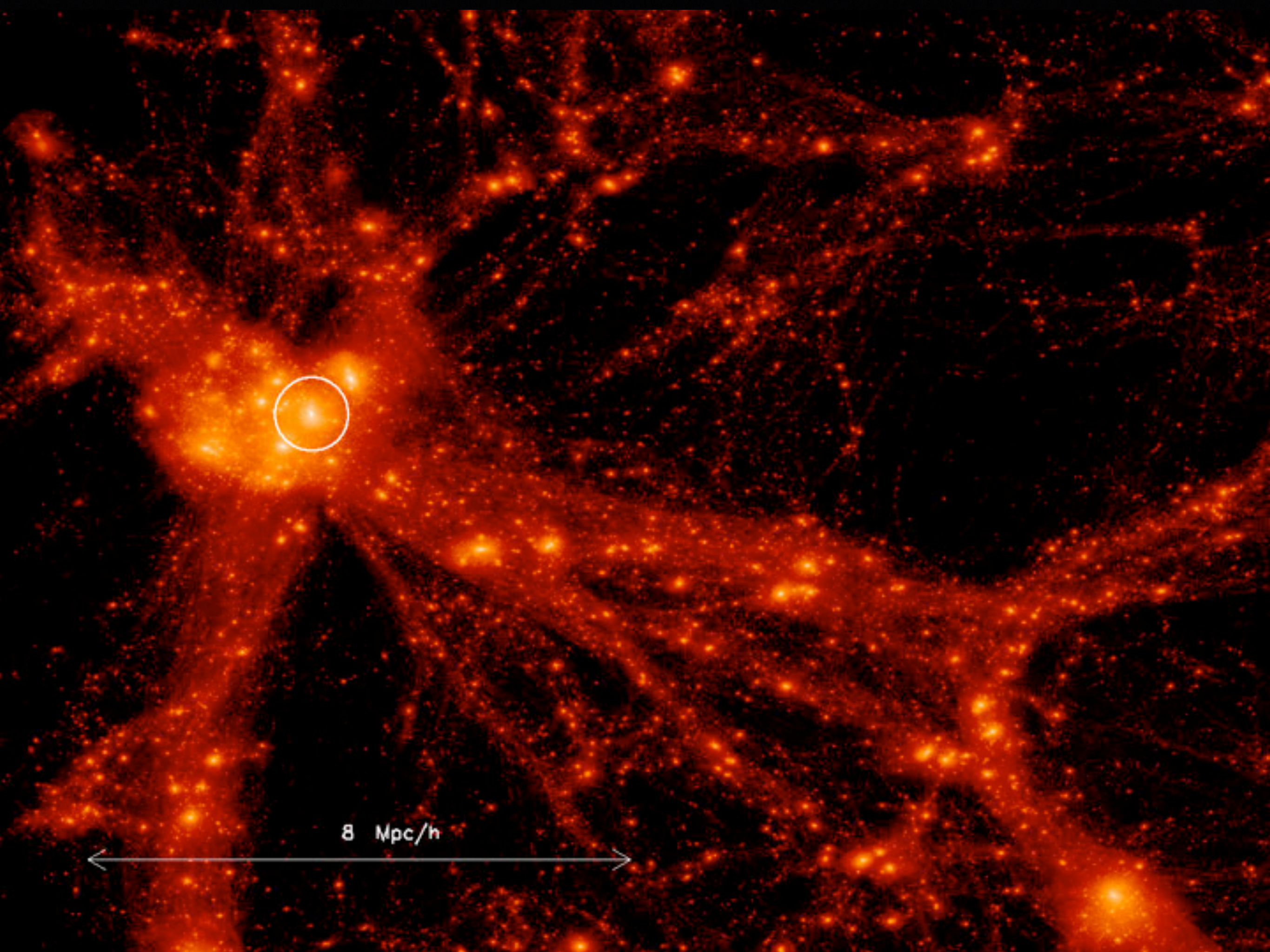


62 Mpc/h Bolshoi



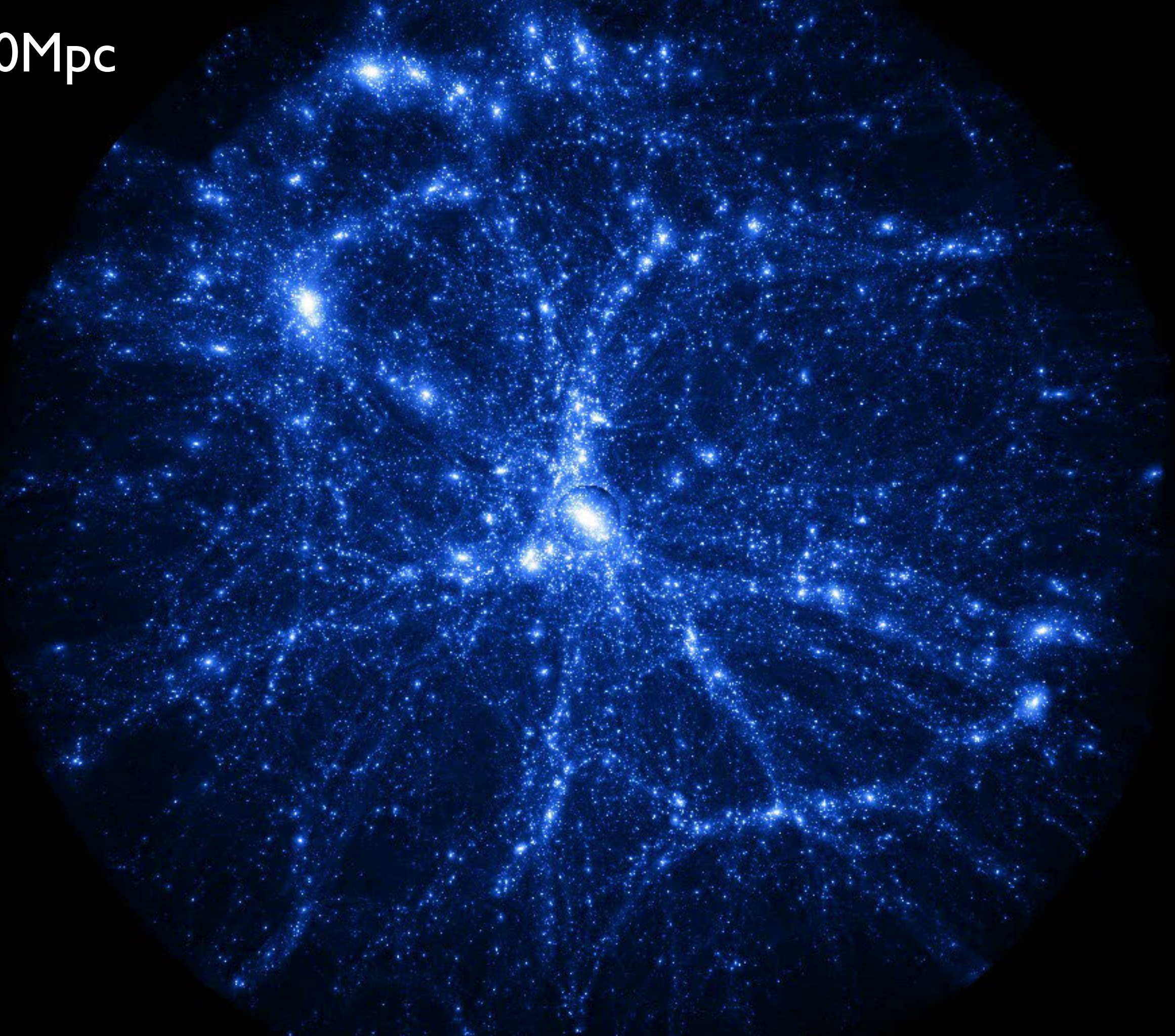
31 Mpc/h Bolshoi





8 Mpc/h

20Mpc



Zeldovich Approximation

If initial fluctuations are smooth, we can estimate the moment of collapse and the whole dynamics of the collapse without assuming the spherical symmetry or any kind of homogeneity of initial density perturbations as we did for the spherical infall model or for the homogeneous ellipsoid model. In the Zeldovich approximation we follow the motion of a fluid element. This is done using the Lagrangian approach to the equations of hydrodynamics.

$\vec{r} =$ proper coordinate, changes with time
 $\vec{x} =$ comoving coordinate, changes with time
 $\vec{q} =$ lagrangian coordinate, does not depend on time

If we know comoving coordinates, we always can find proper coordinates using :

$$\vec{r} = a(t) \vec{x}(t)$$

$\vec{q} =$ lagrangian coordinate is a label of particles. This is comoving coordinate of particle in the absence of perturbations

According to Zeldovich (1970) the relation between $\vec{x}(t)$ and \vec{q} is given by:

$$\vec{x}(t) = \vec{q} + b(t) \vec{S}(\vec{q})$$

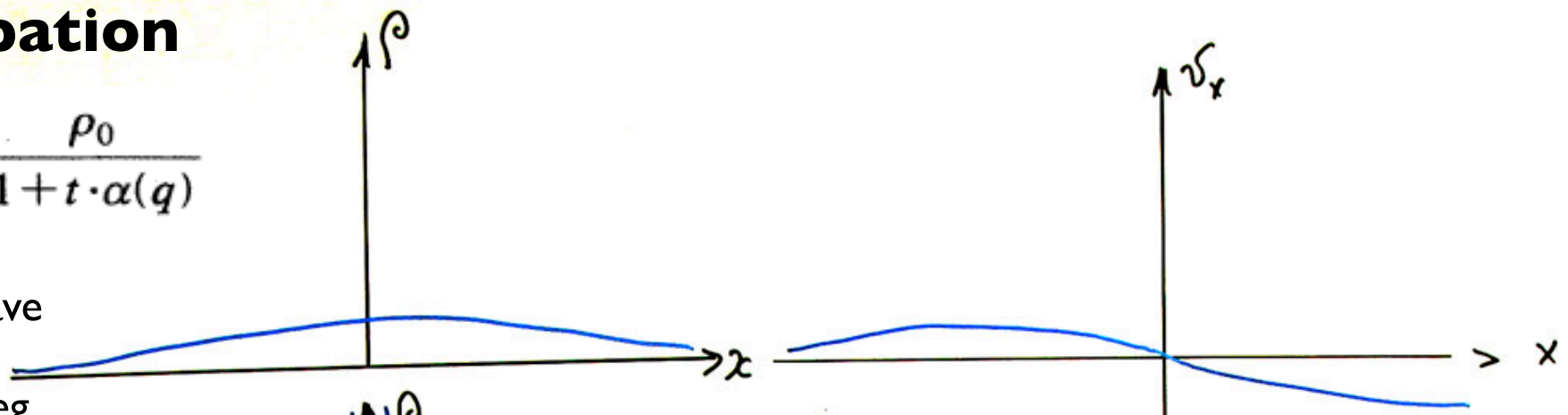
Here $b(t)$ = growth rate of fluctuations in the linear regime (= $a(t)$ for a flat CDM universe)

$\vec{S}(\vec{q})$ is a displacement vector. Note that it does not depend on time

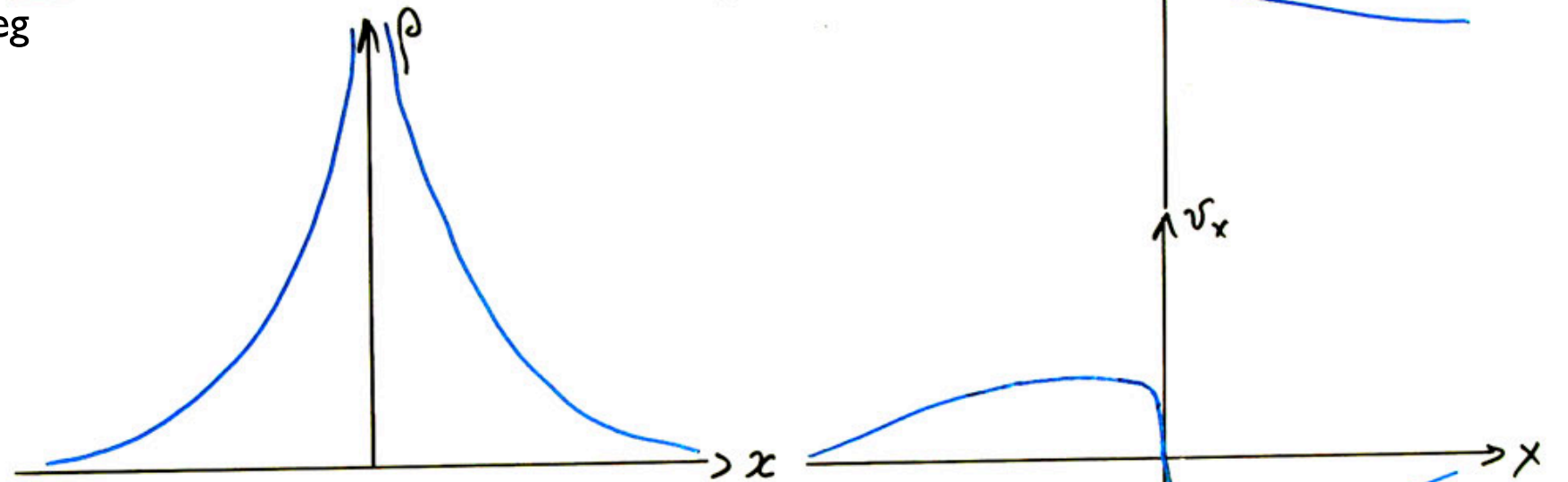
Evolution of a 1D perturbation

$$x(q,t) = q + t \cdot v_0(q) \quad \rho(q,t) = \frac{\rho_0}{1 + t \cdot \alpha(q)}$$

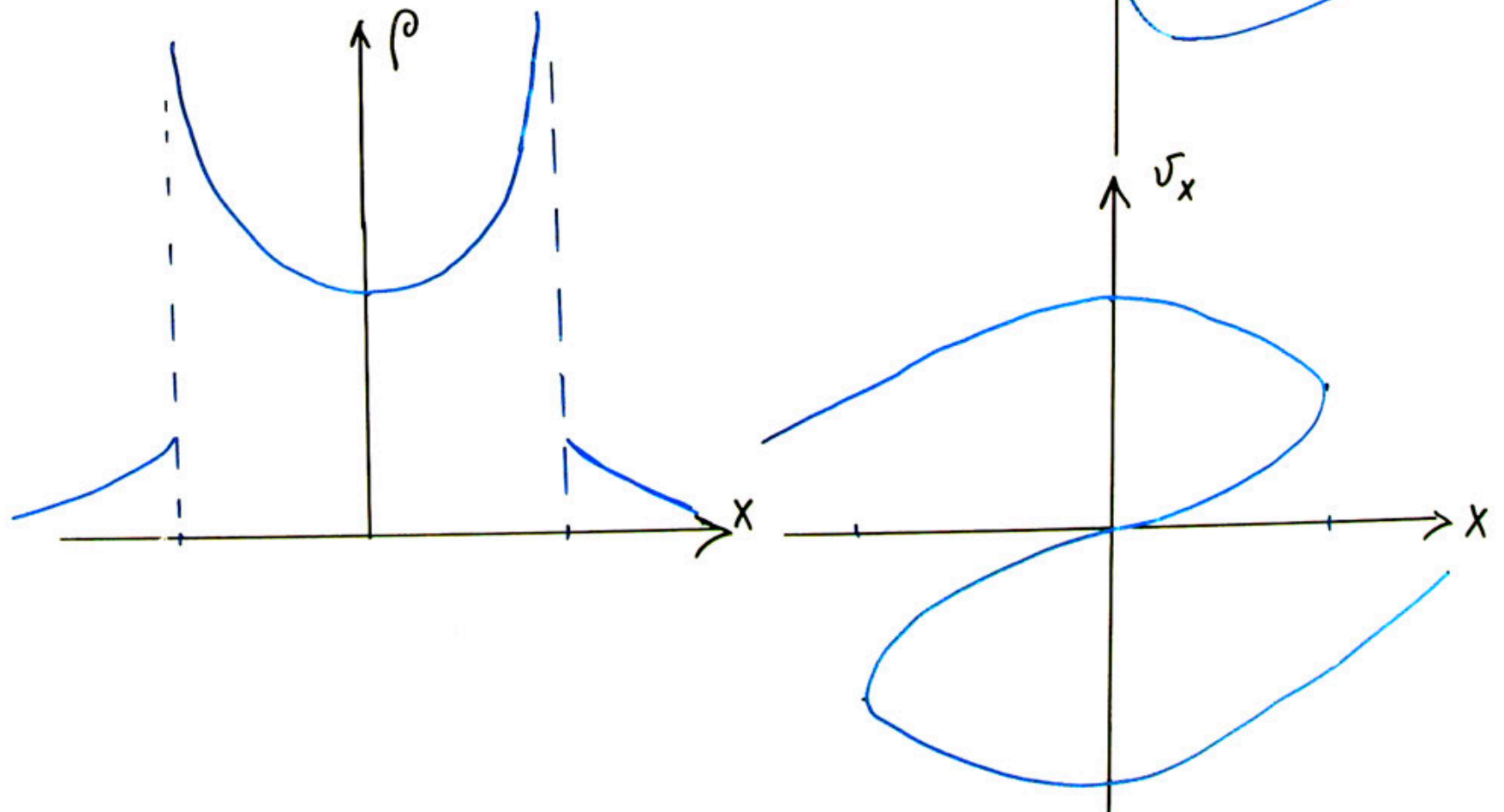
Early stages of evolution: small-amplitude wave produces an overdensity around $x=0$. Perturbation in velocity goes in phase (90 deg difference) with the density perturbation



Formation of caustic: density is infinite at $x=0$. The curve of $V(x)$ has vertical slope at the same $x=0$ distance.

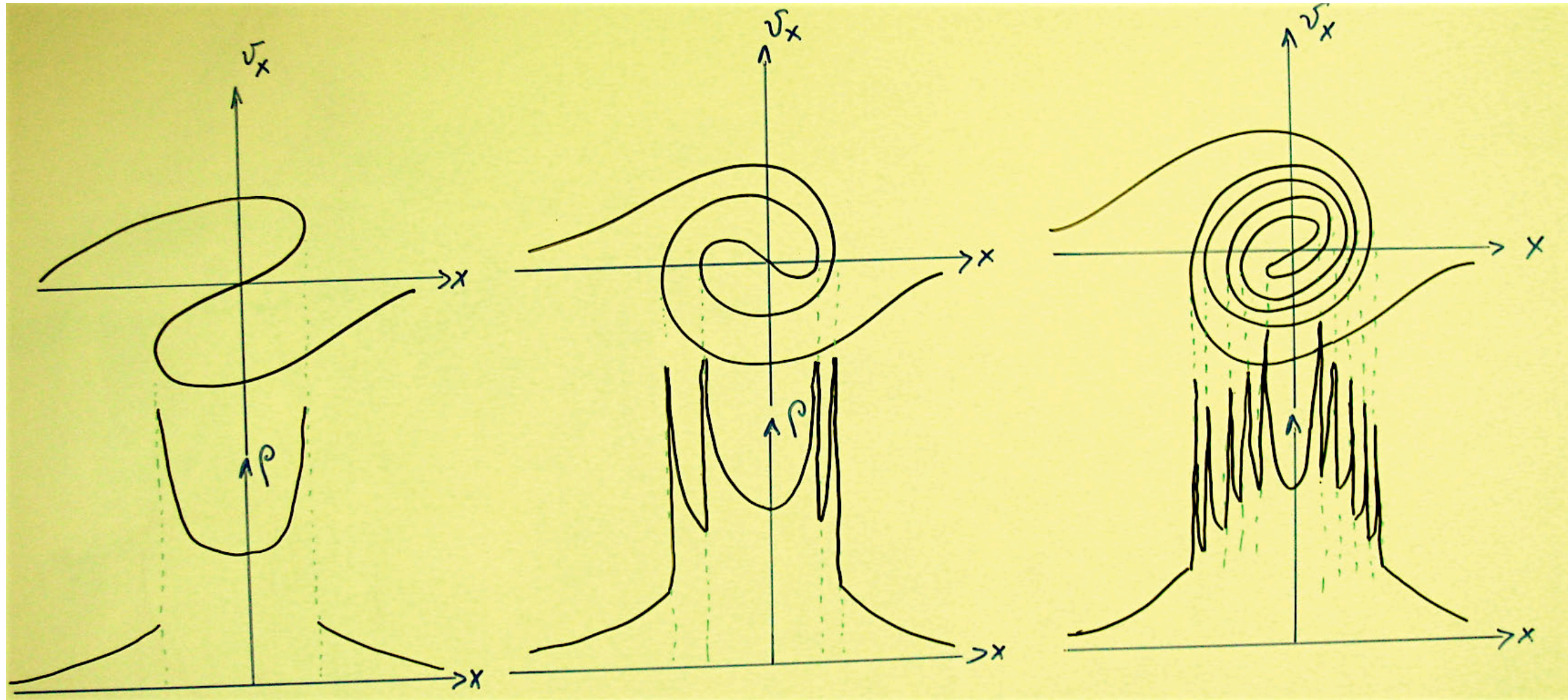


At later stages particles still keep moving along their initial direction: they do not turn around in the Zeldovich approximation. Now we have two caustics, which move away from the central $x=0$ plane. At each point inside the region of the caustics there are three flows.

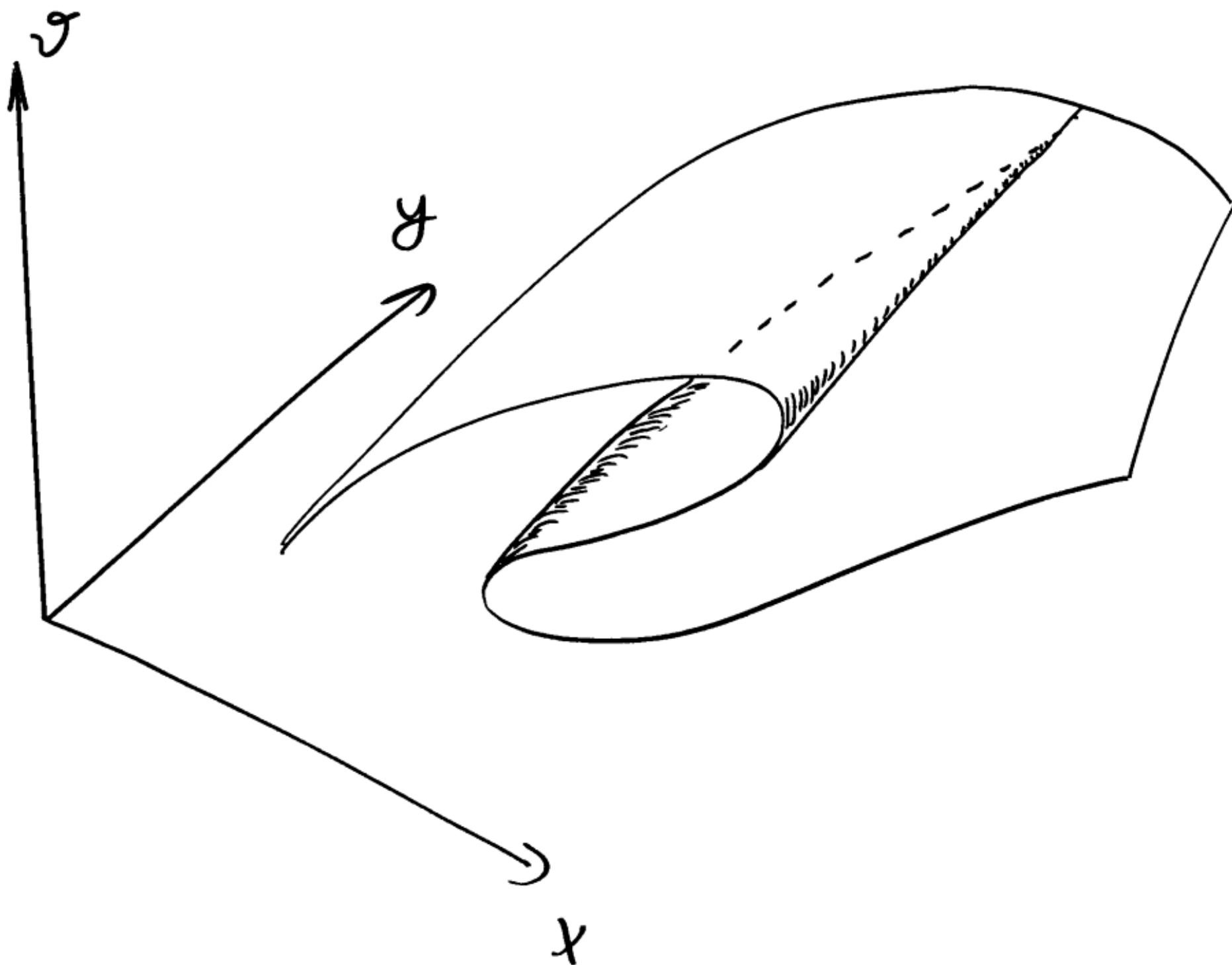


Evolution of a 1D perturbation: beyond Zeldovich approximation

In reality, particles will move away from the center for a short while, then turn around and fall back. This produces a more complicated picture illustrated below. Each folder in the velocity space produces two caustics in real space. At each point in real space there are odd number of flows: 1, 3, 5...

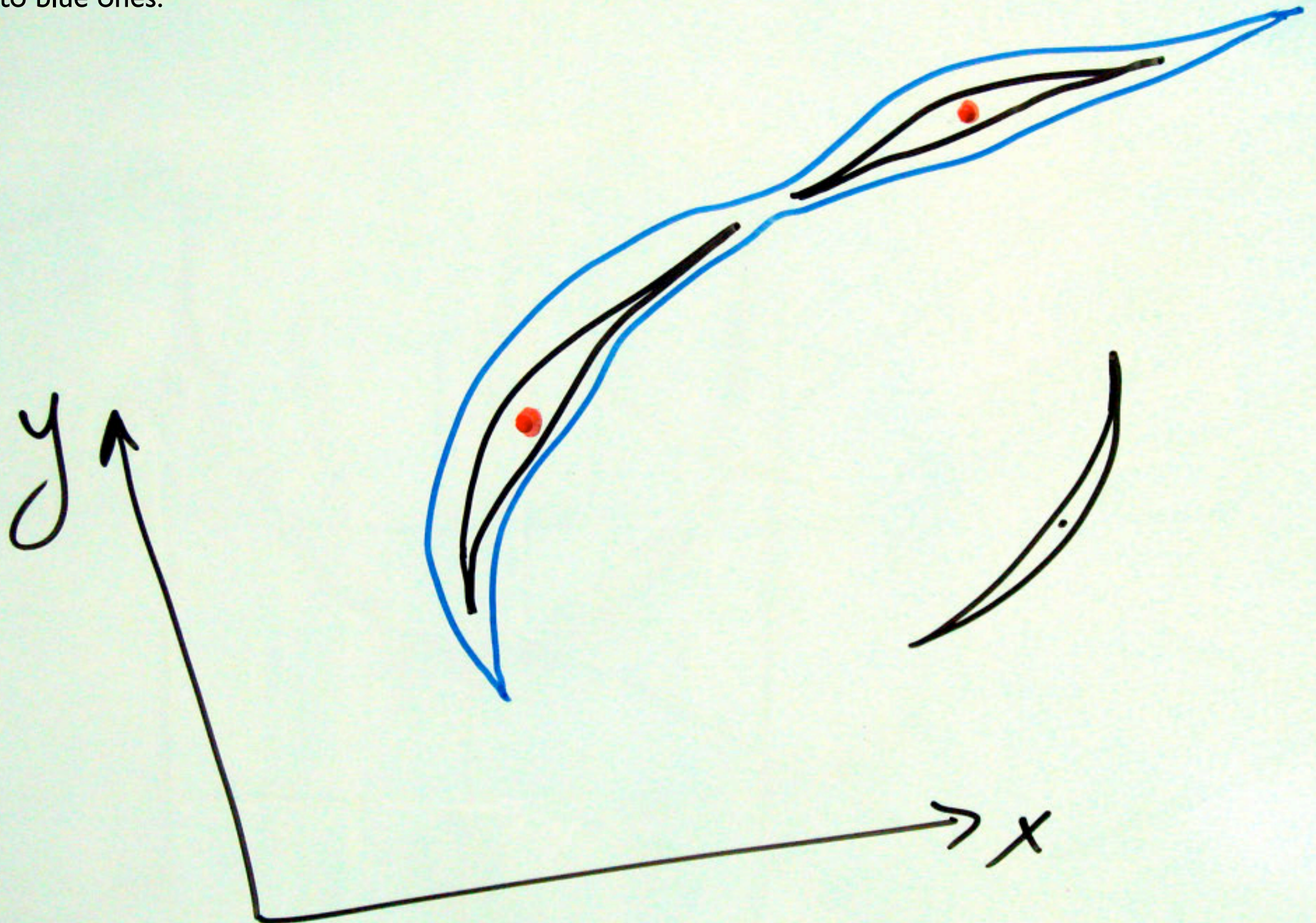


In 2 dimensions:

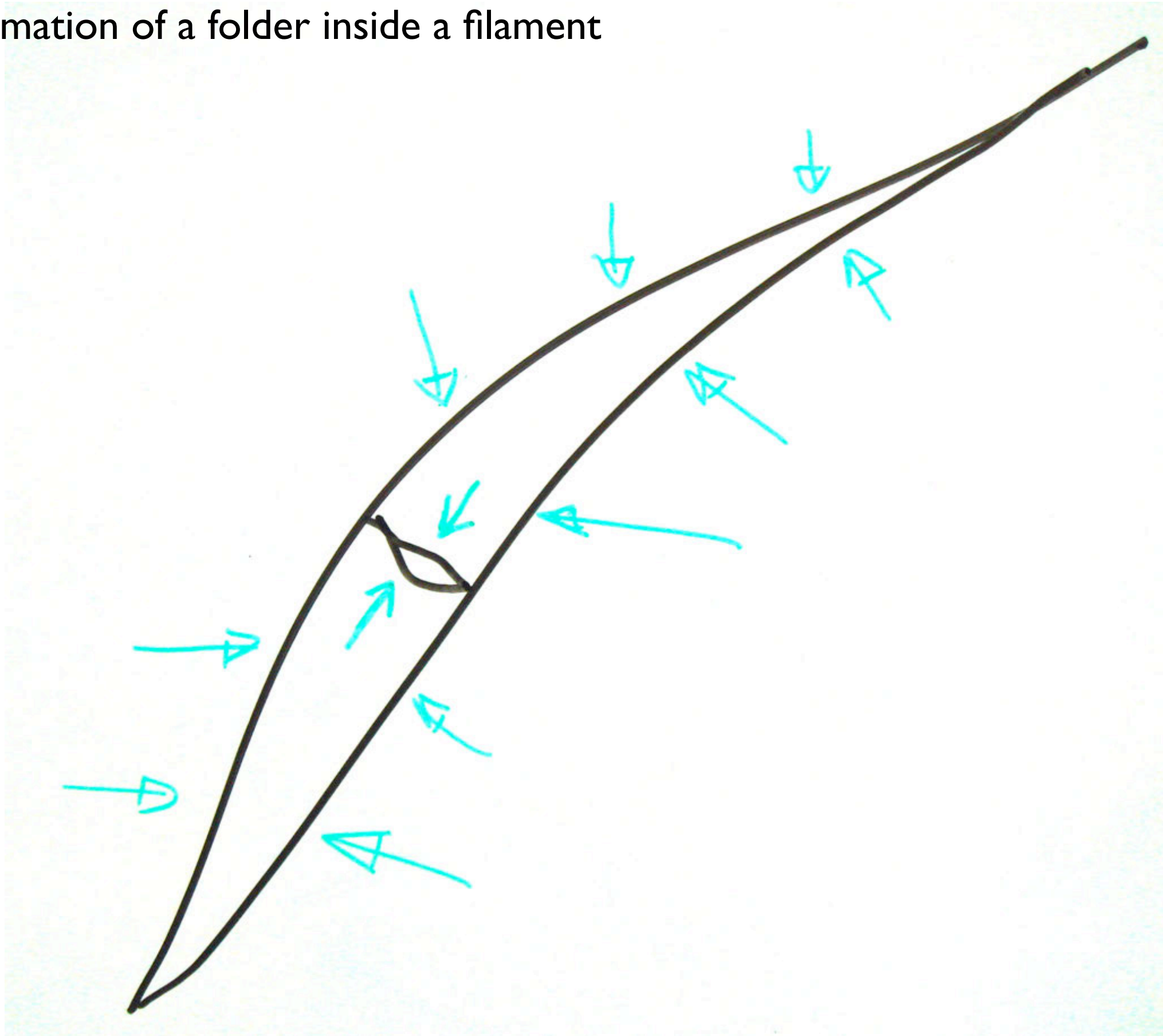


In 2 dimensions: how filaments join - no crossing. They continue smoothly from one to another.

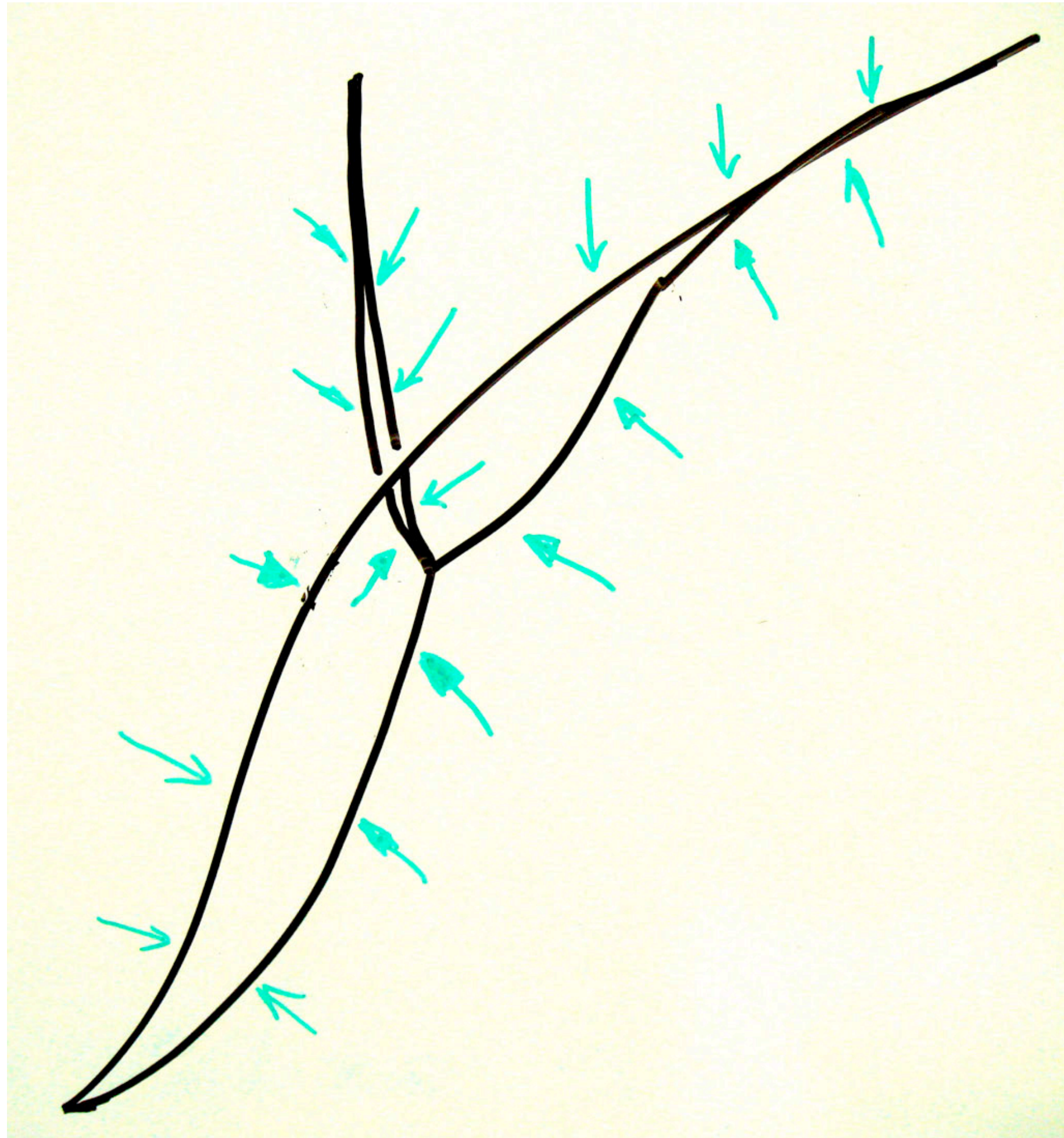
First singularities start in red points. Then they grow to black curves and then to blue ones.



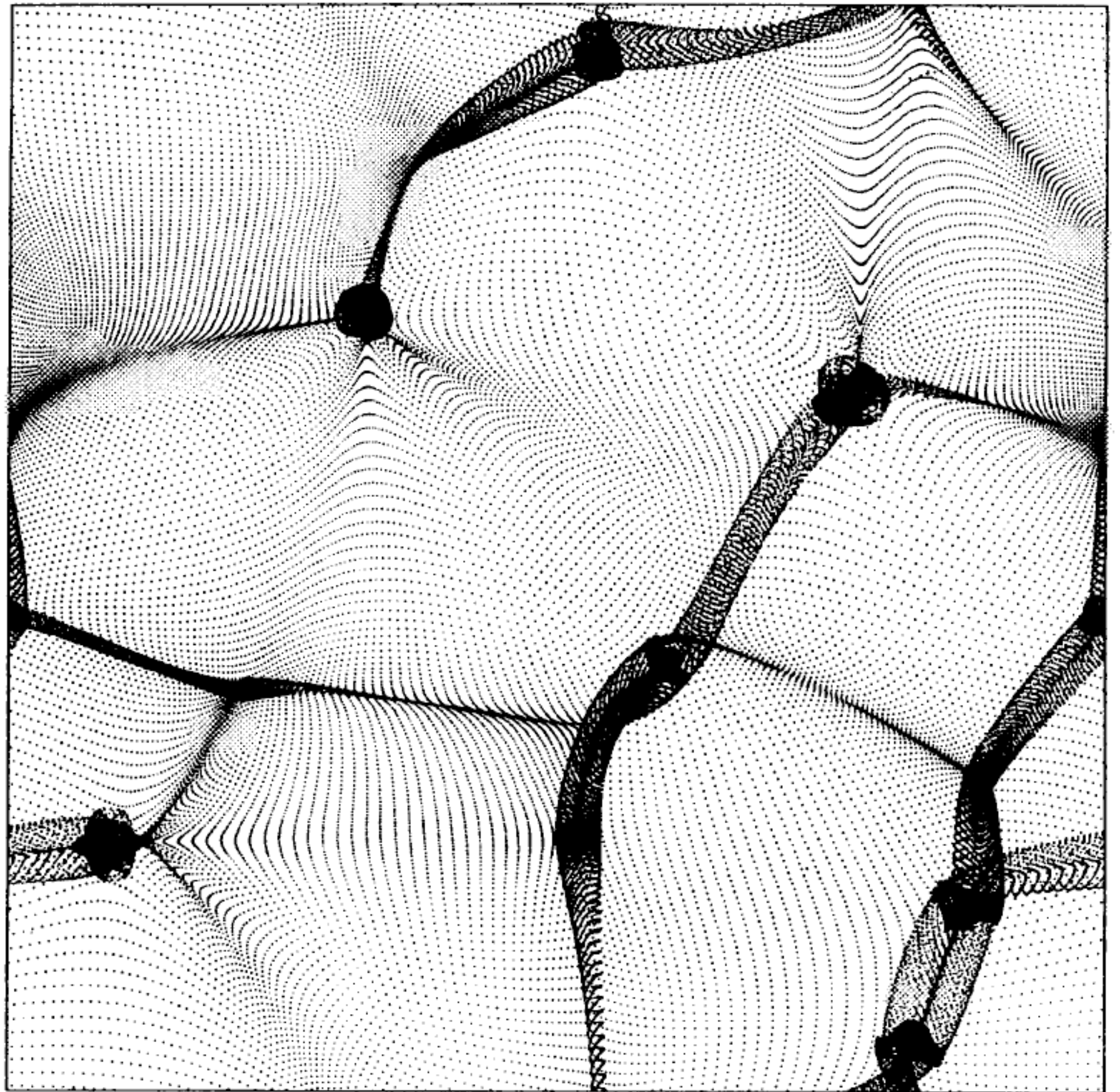
In 2 dimensions: formation of a folder inside a filament



In 2 dimensions:
branching filaments due
to converging flow along
filaments

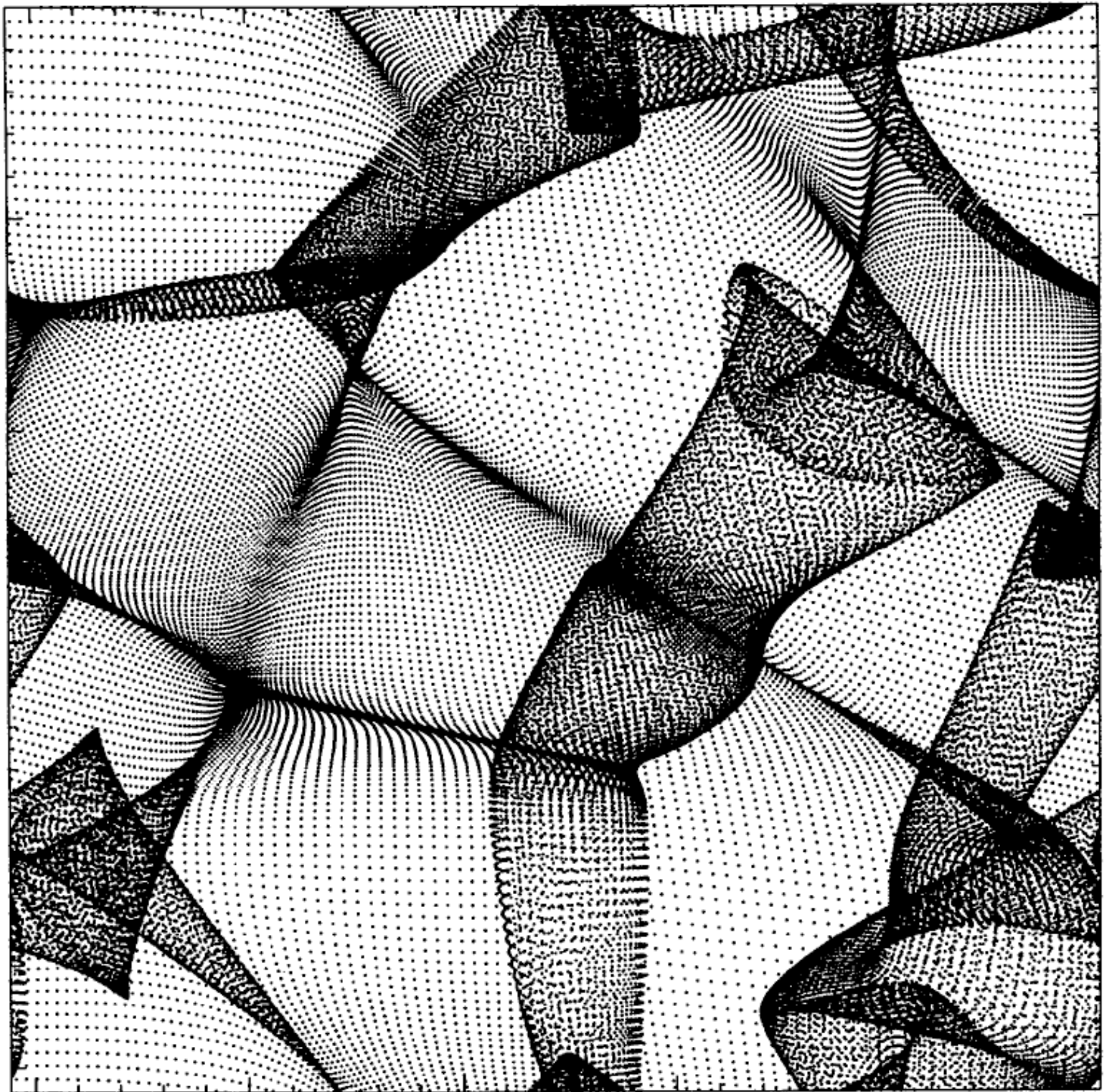


Formation of caustics
in a simplified 2D
model, which has
only very few long-
wave harmonics

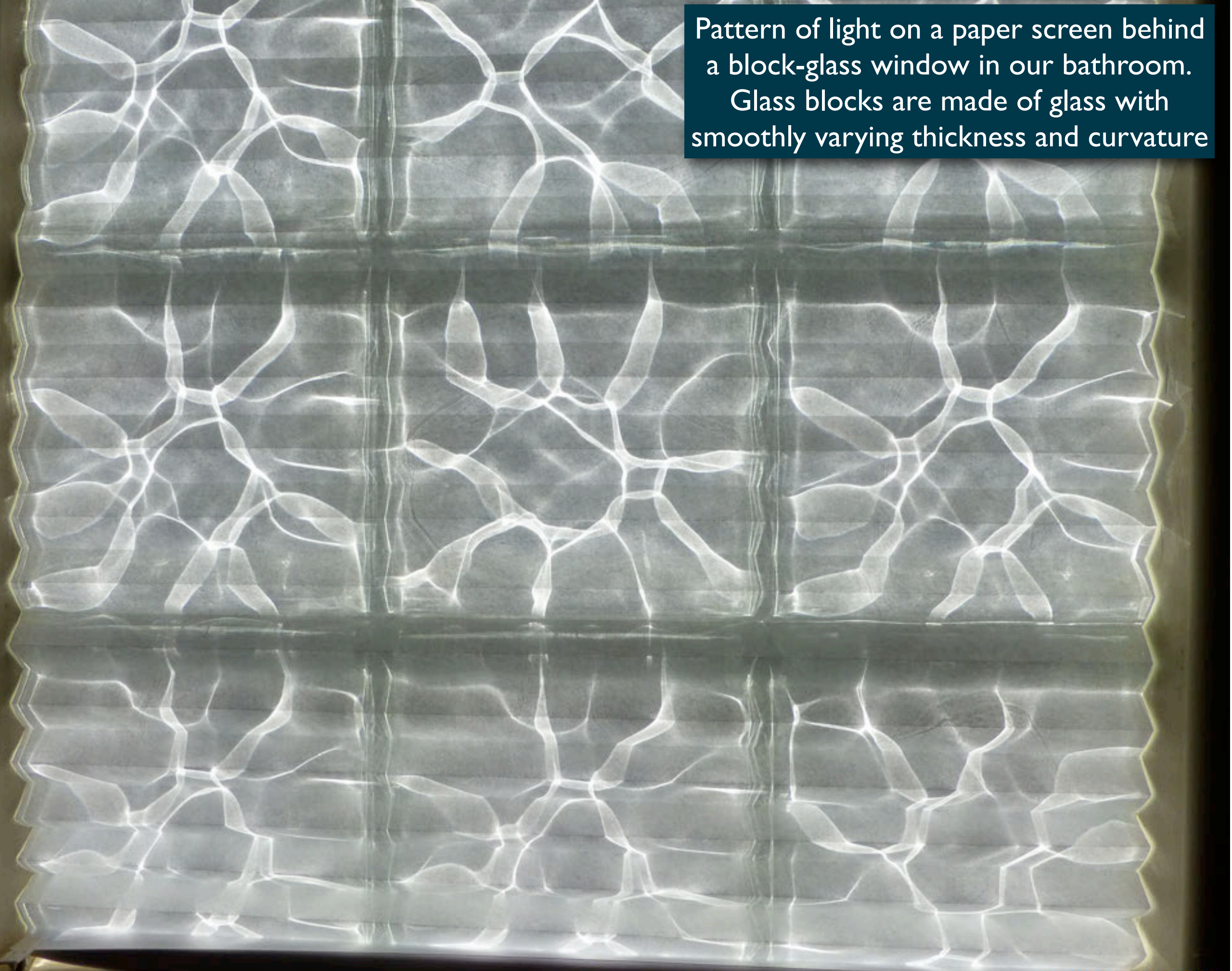


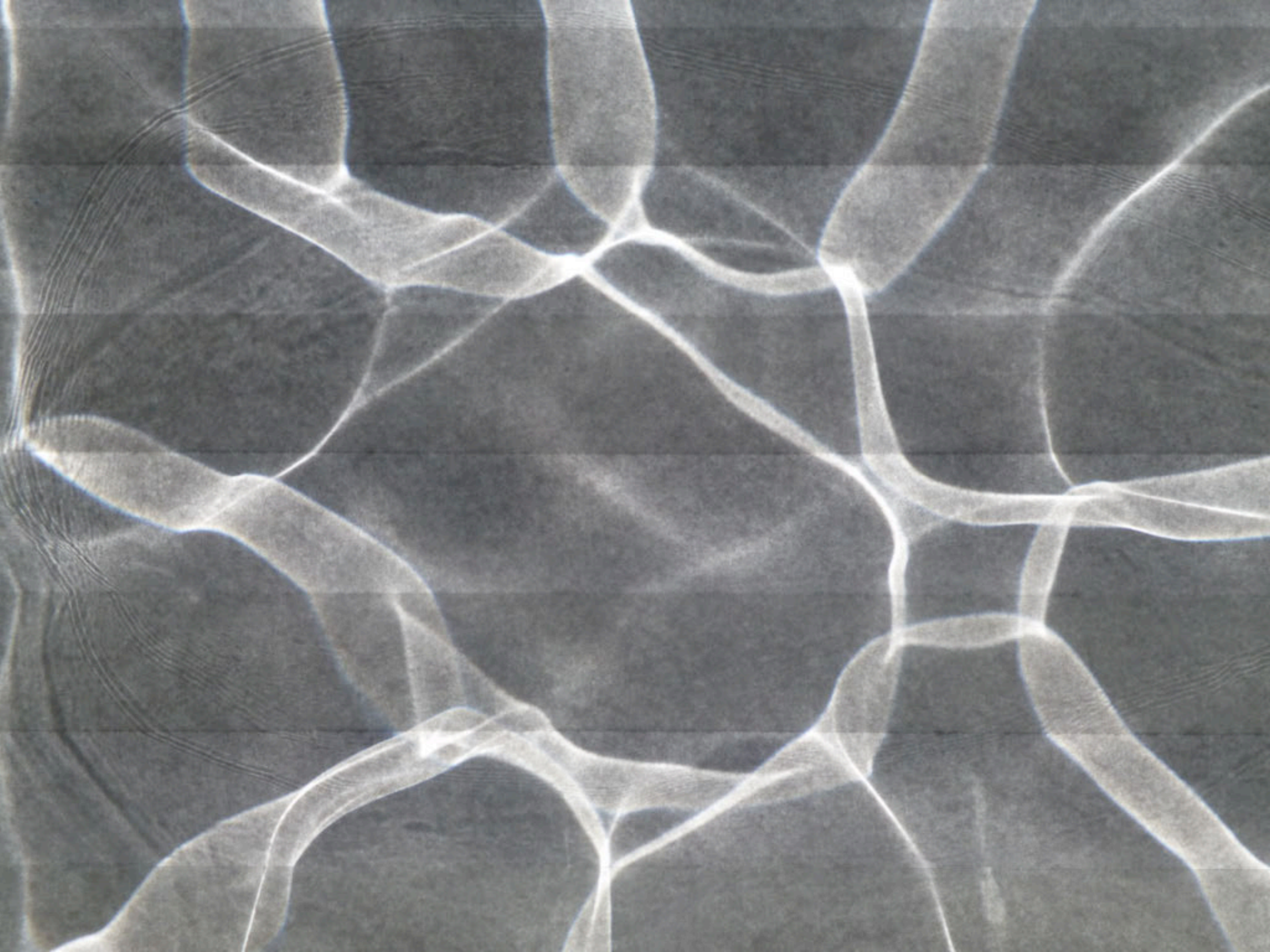
Sahni et al 1994

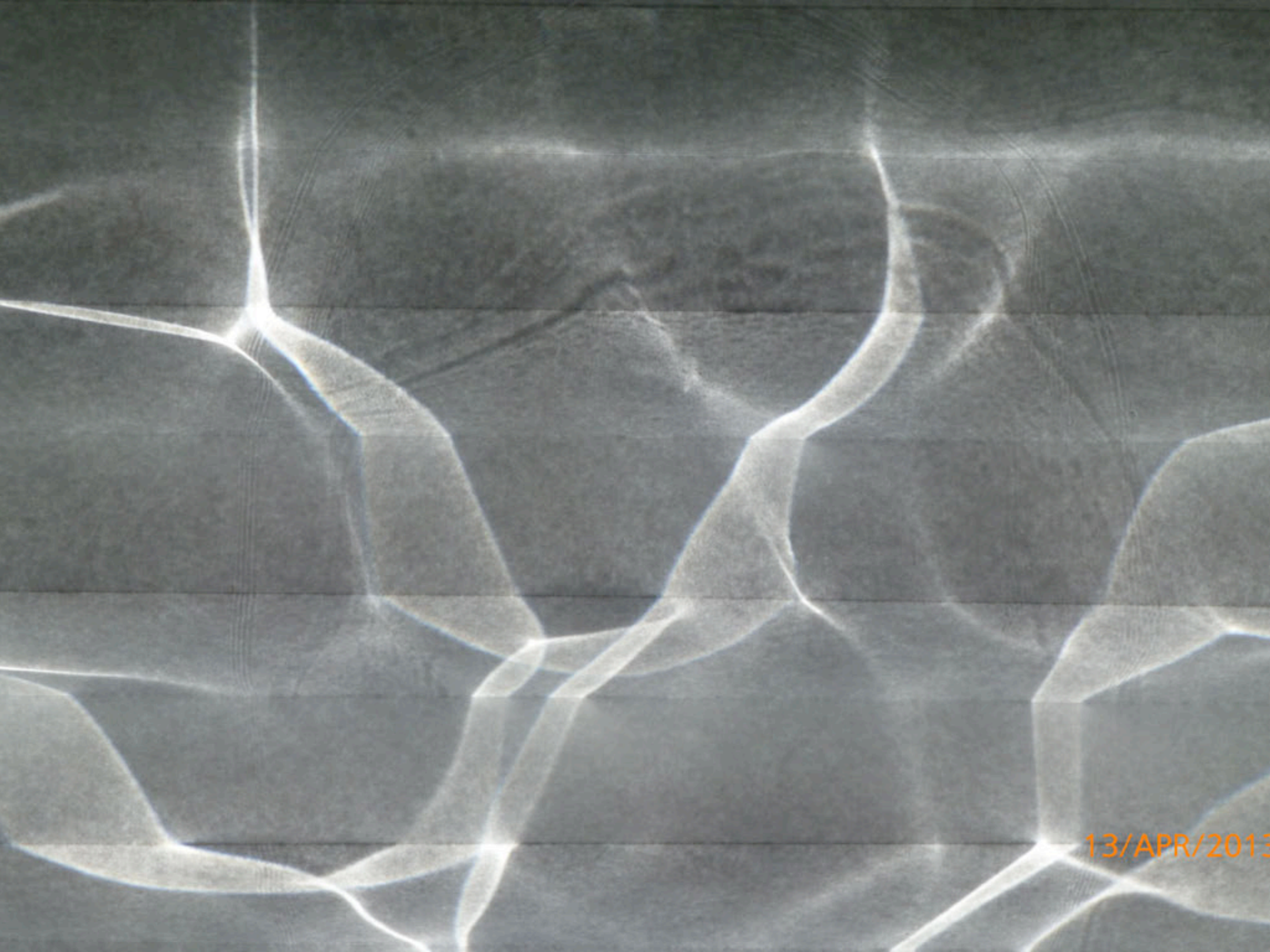
At later moments particles start to fly through regions of high density. This is where the Zeldovich approximation badly fails.



Pattern of light on a paper screen behind a block-glass window in our bathroom. Glass blocks are made of glass with smoothly varying thickness and curvature

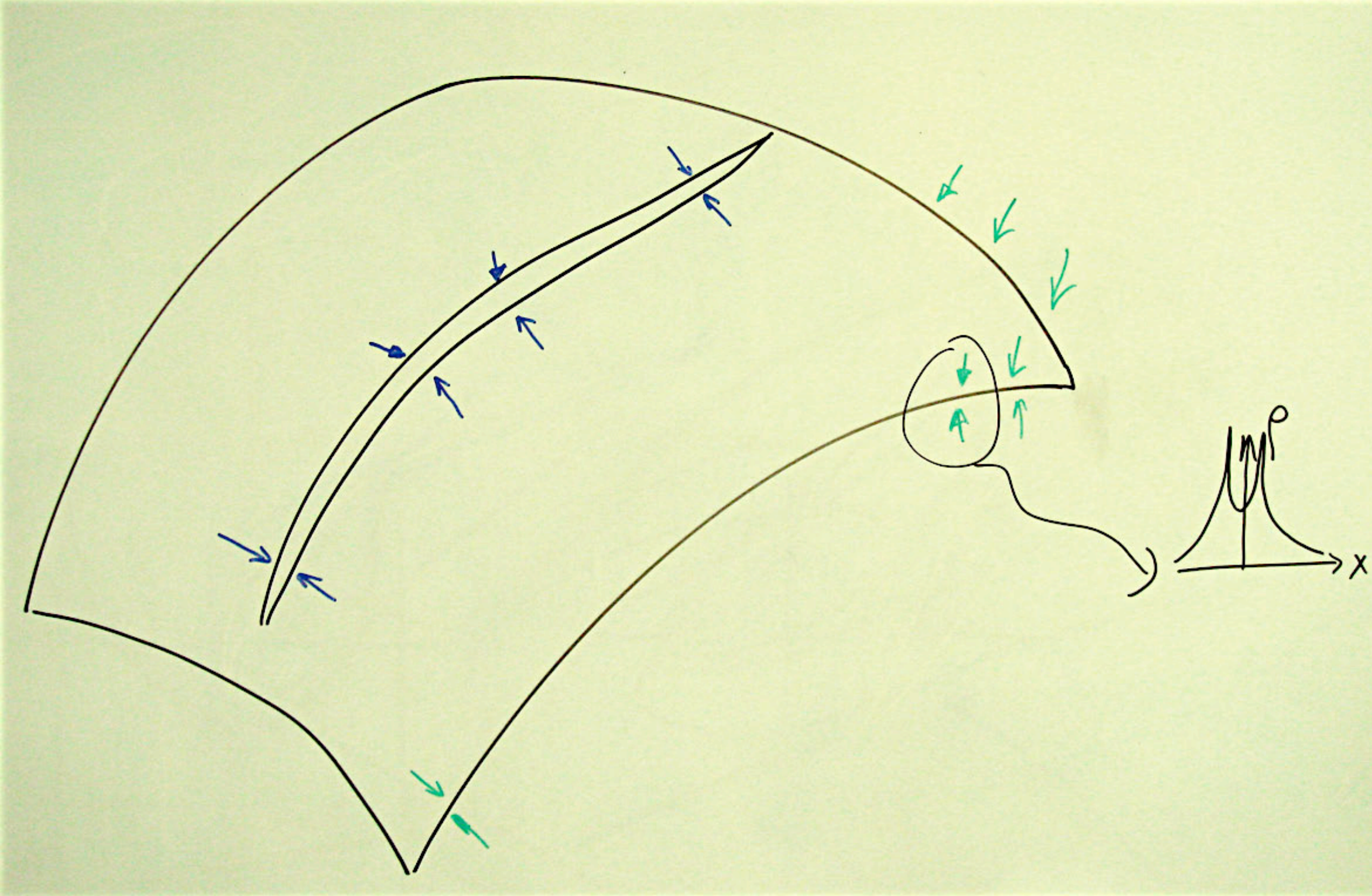




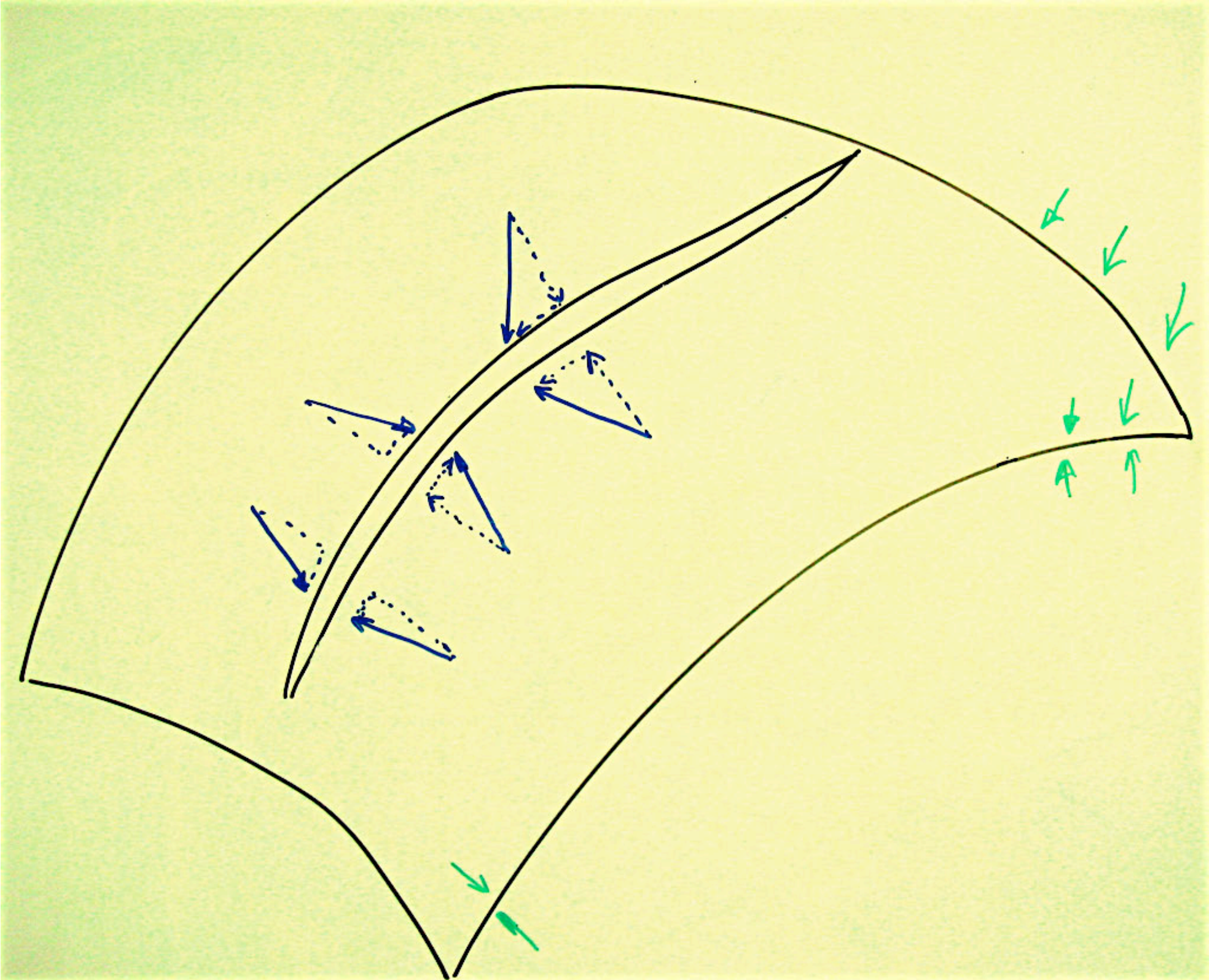


13/APR/2013

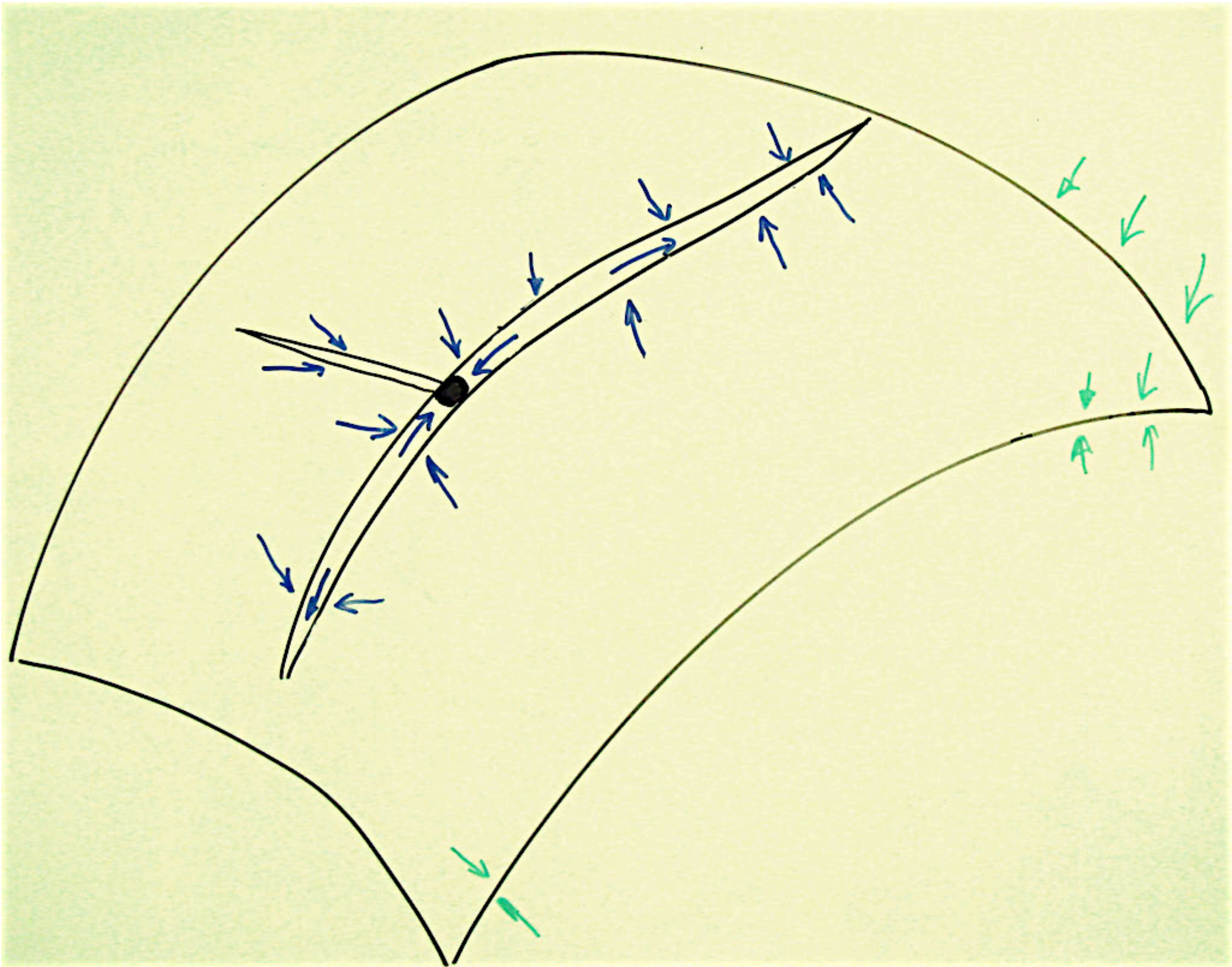
3 dimensions:



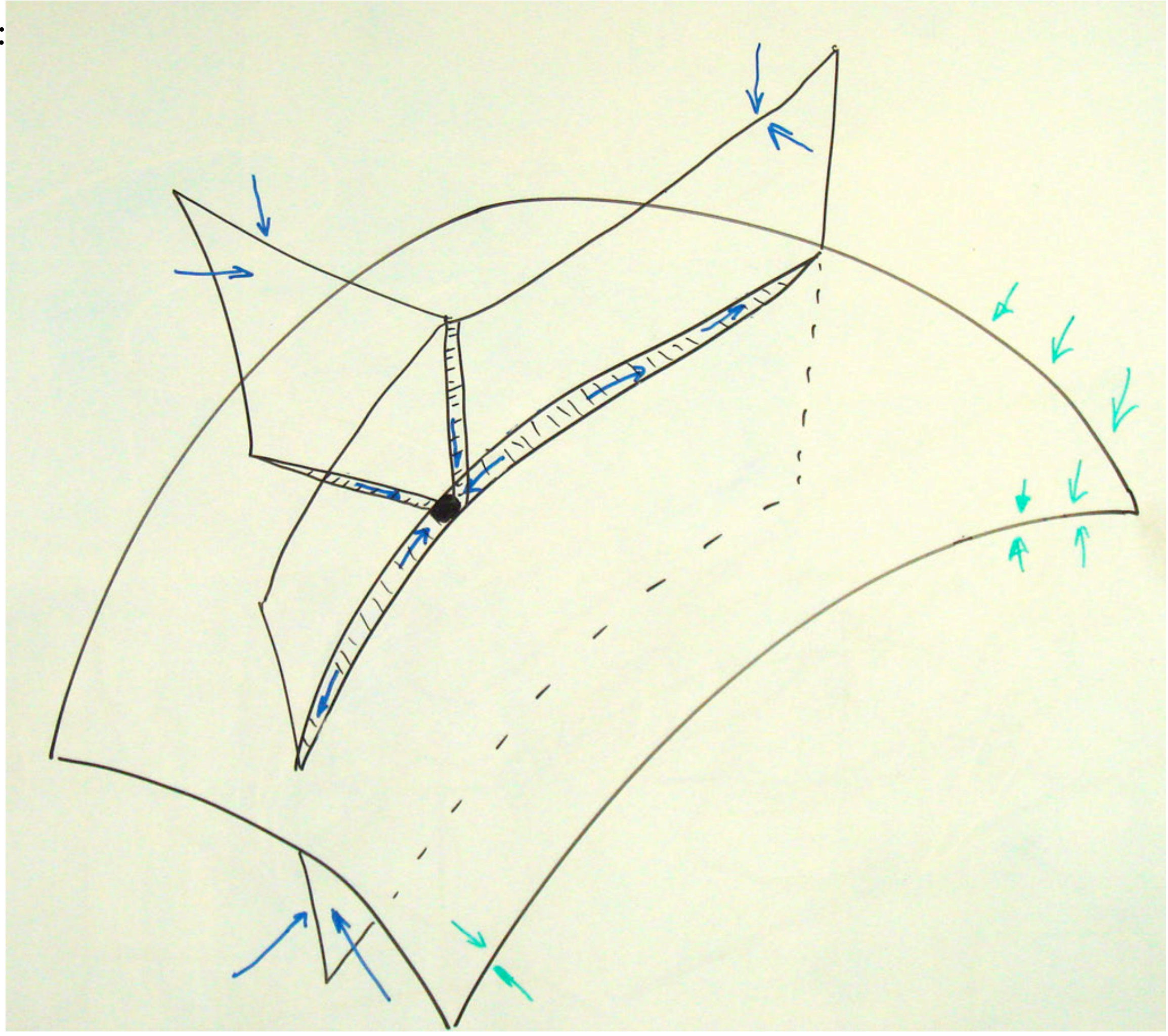
3 dimensions:

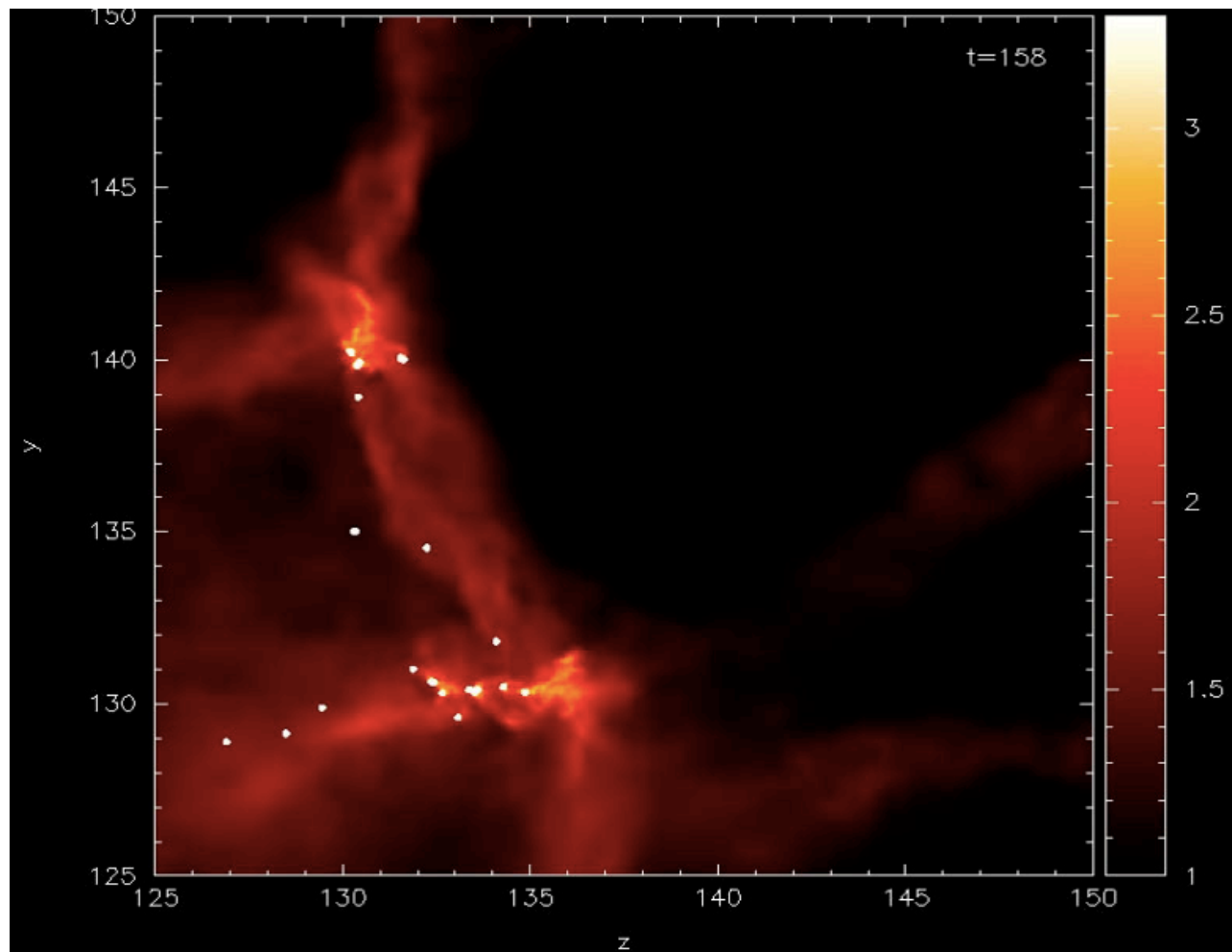
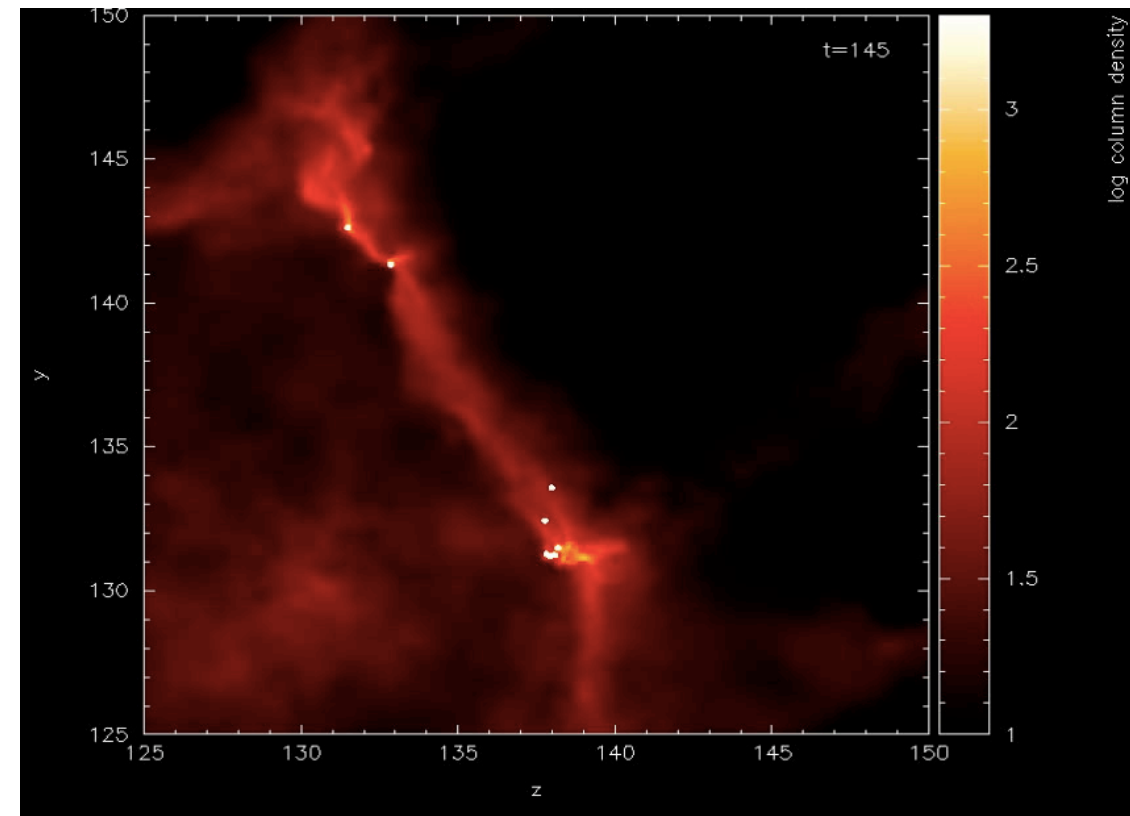
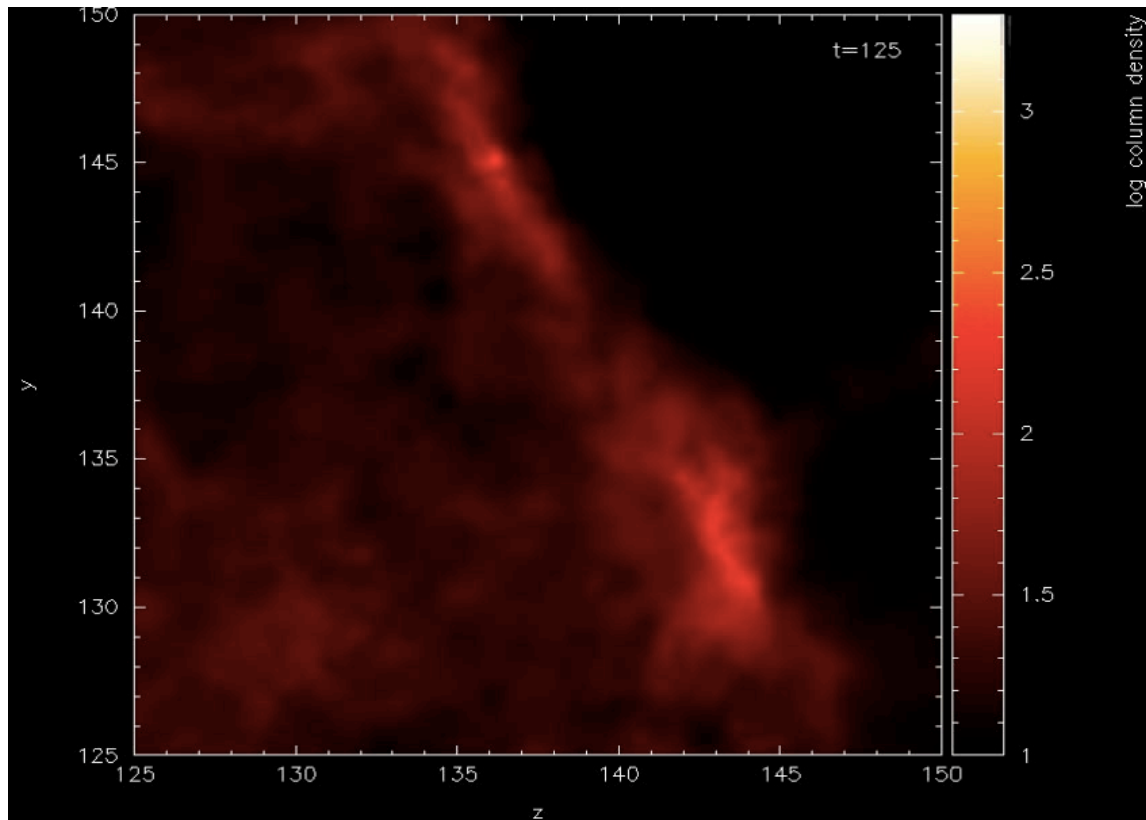


3 dimensions:



3 dimensions:





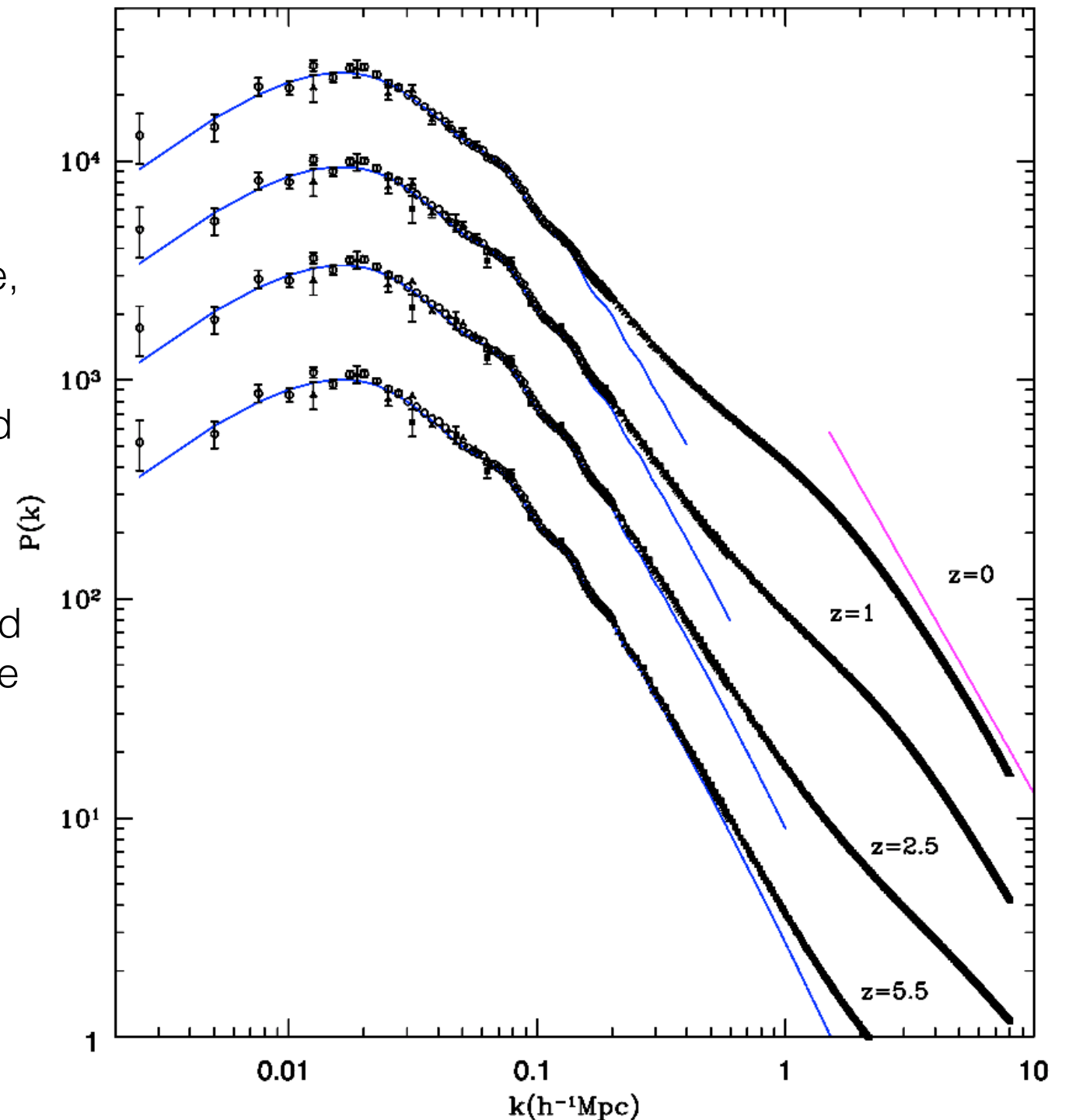
Column density plot of Cloud 1 in the y - z plane at $t = 19.1$ Myr, integrating over the central 16 pc along the x -direction. The dots show the stellar objects (sink particles). The electronic version of this figure shows an [animation](#) of this region from $t = 16.6$ to 19.9 Myr. The column density is in code units, which correspond to $9.85 \times 10^{19} \text{ cm}^{-2}$.

Model of star formation in Molecular clouds

Evolution of the power spectrum of dark matter.

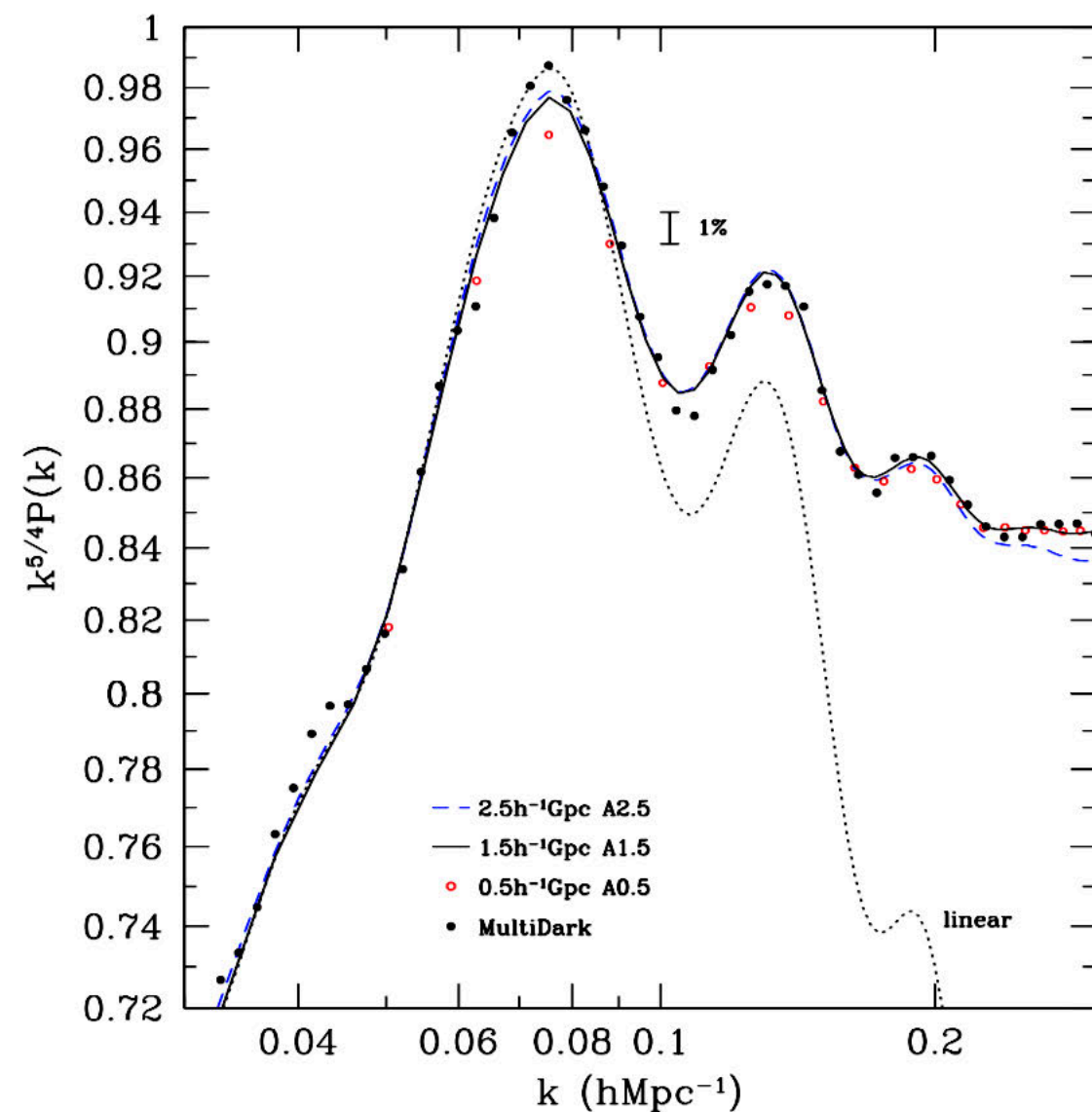
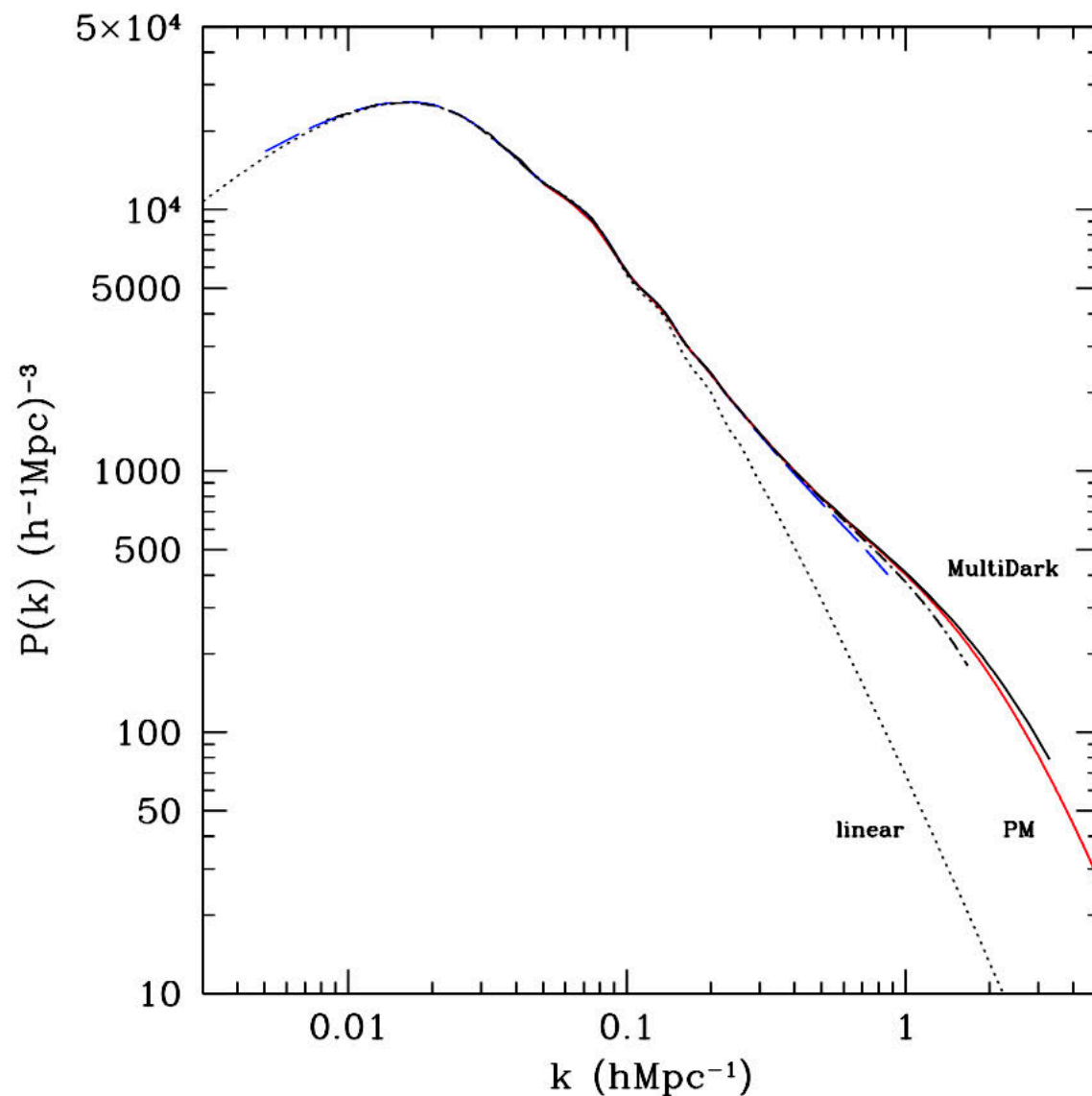
three regimes:

- linear regime: fluctuations increase the amplitude, but shape of $P(k)$ is the same
- mildly nonlinear regime: fluctuations collapse and amplitude grows faster than in linear regime. Shape evolves with time.
- Deep nonlinear regime: dark matter has collapsed into virtualized dark matter halos that do not change their physical interior mass. In comoving coordinates they get smaller as universe expands.

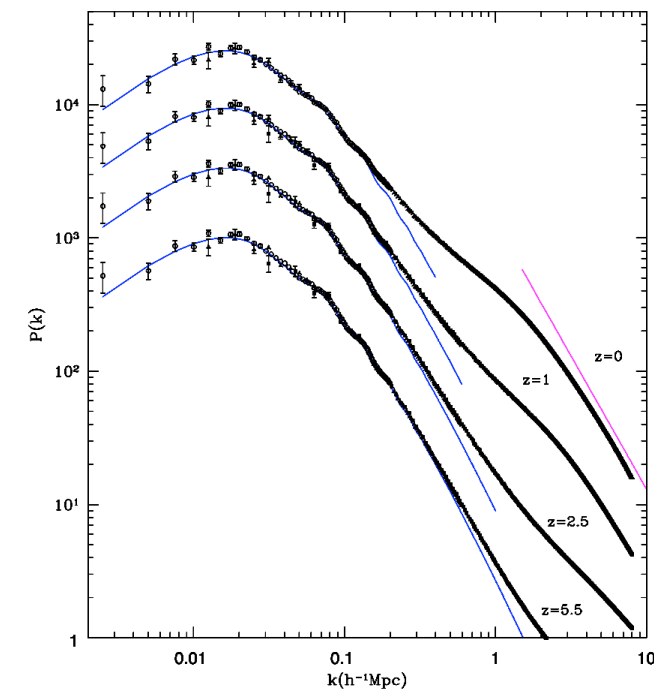
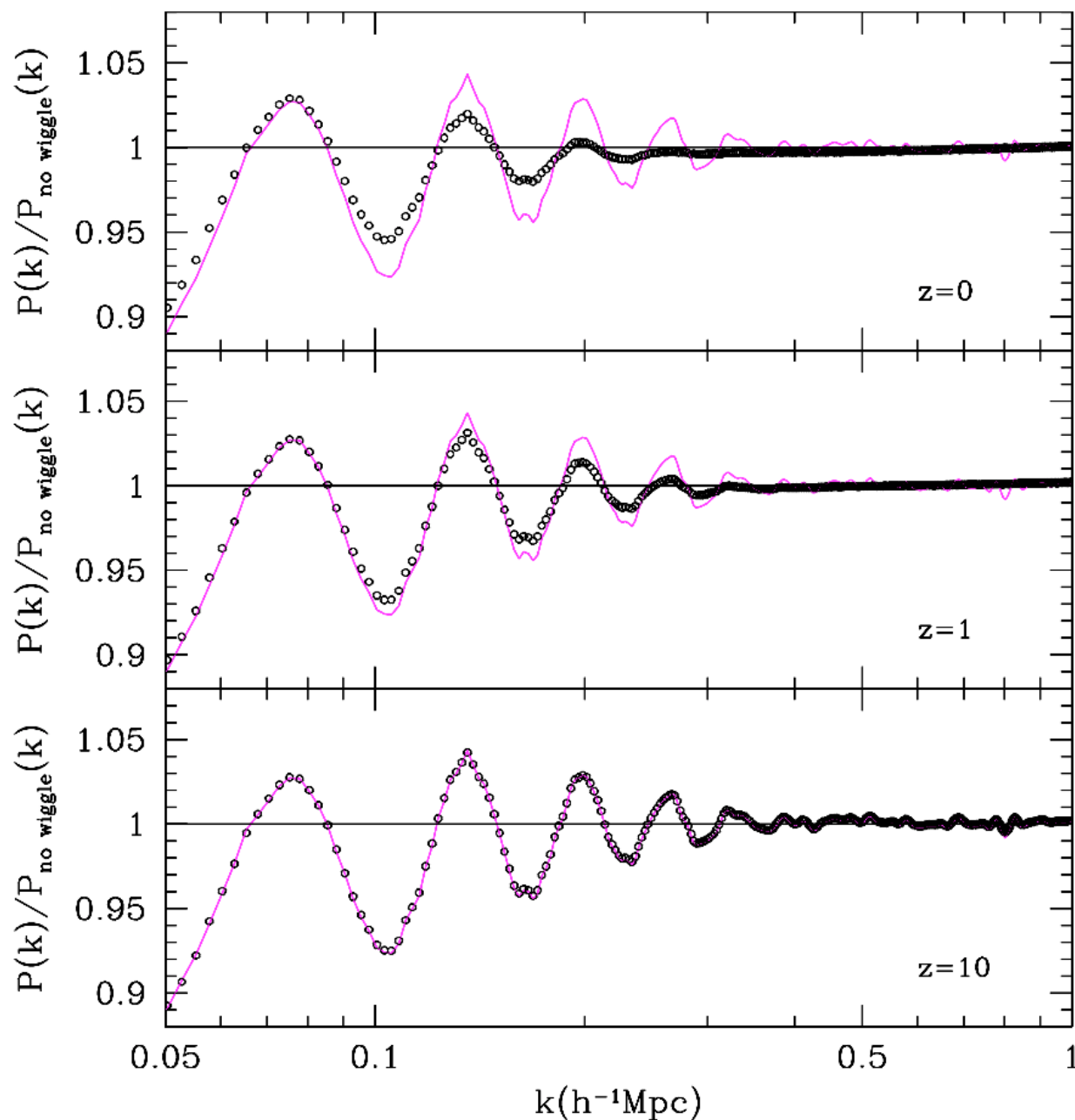


Evolution of the power spectrum of dark matter.

- linear regime: fluctuations increase the amplitude, but shape of $P(k)$ is the same
- mildly nonlinear regime: fluctuations collapse and amplitude grows faster than in linear regime. Shape evolves with time.
- Deep nonlinear regime: dark matter has collapsed into virtualized dark matter halos that do not change their physical interior mass. In comoving coordinates they get smaller as universe expands.

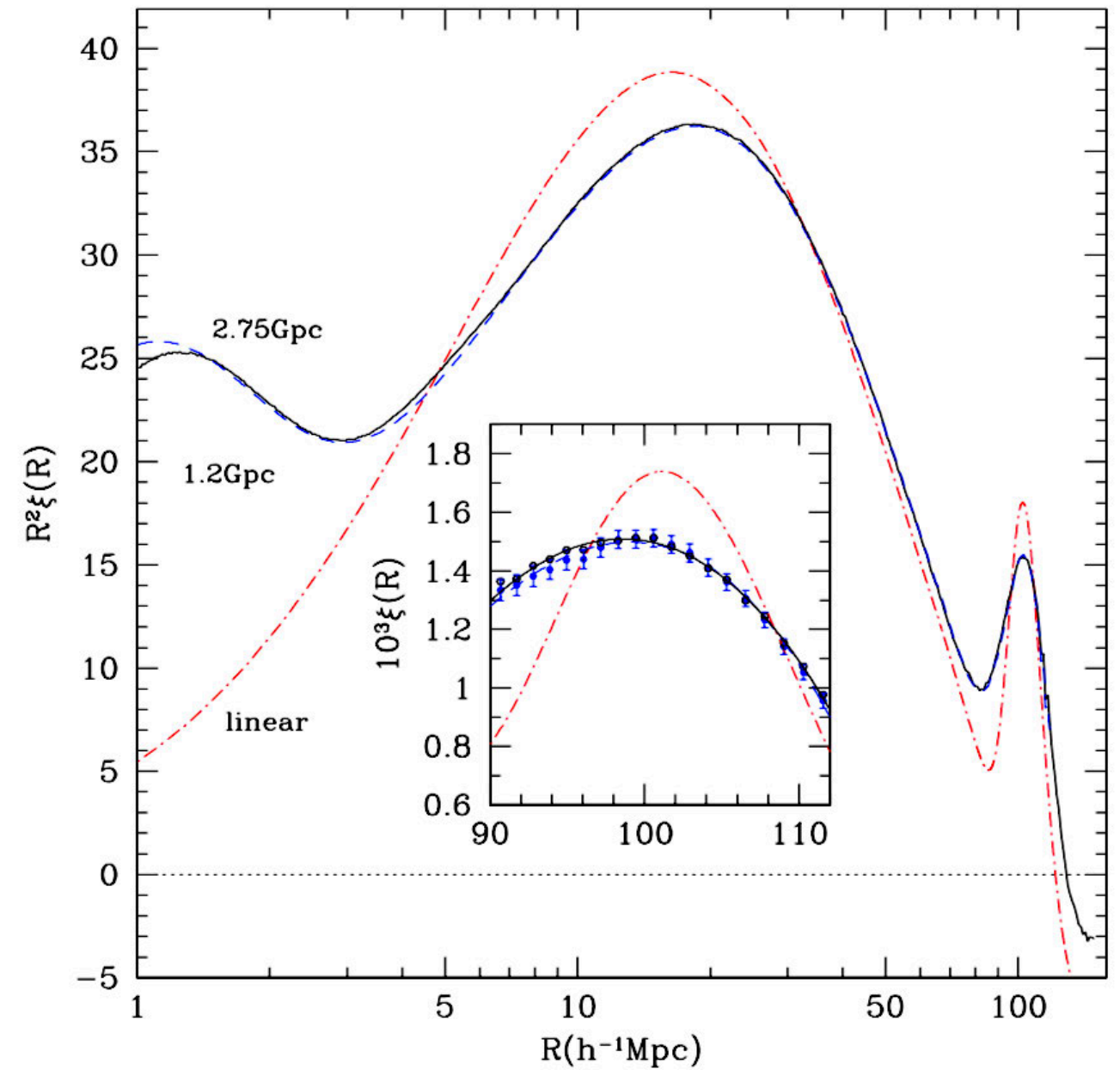
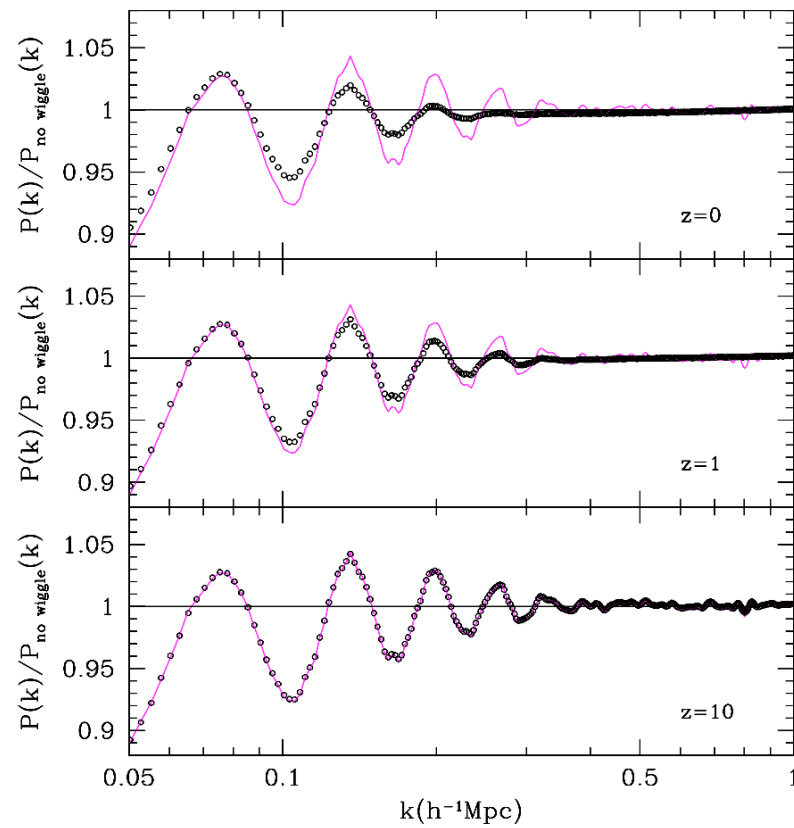


Evolution of BAO wiggles: dumping and shift due to (weak) non-linear gravitational coupling of modes. Effect is small, but is important when we use BAO features to estimate parameters of the Universe.



Magenta: initial conditions ($z=100$)
circles - results of n-body simulations

Evolution of BAO wiggles: dumping and shift due to (weak) non-linear gravitational coupling of modes. Effect is small, but is important when we use BAO features to estimate parameters of the Universe.



Comparison of nonlinear dark matter correlation functions.

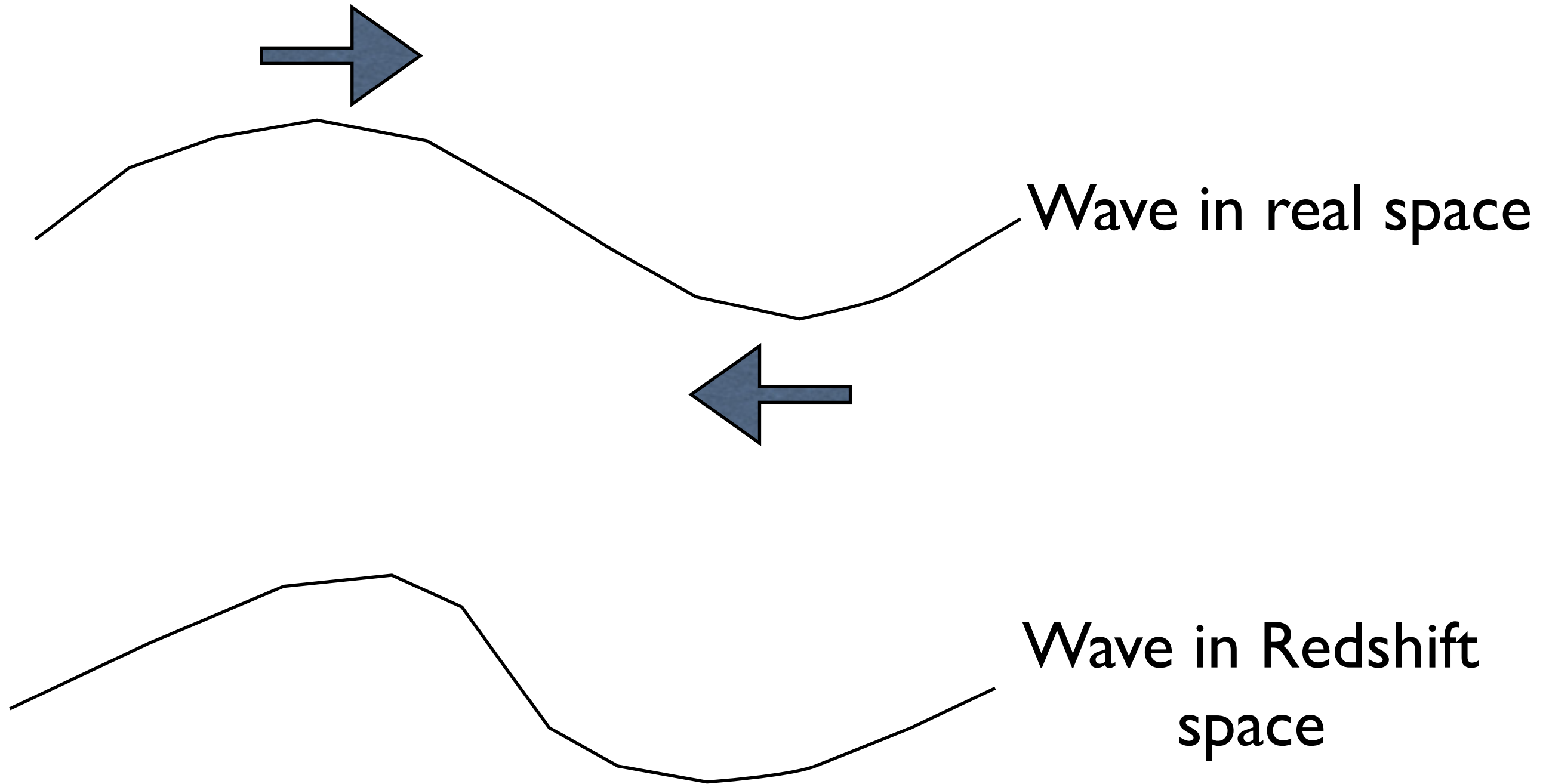
Thus, we get the relation between the correlation function and the power spectrum:

$$\xi(r) = \frac{1}{2\pi^2} \int_0^\infty k^2 dk \frac{\sin kr}{kr} P(k)$$

There is an inverse relation:

$$P(k) = 4\pi \int_0^\infty r^2 dr \xi(r) \frac{\sin kr}{kr}$$

Redshift distortions: long waves



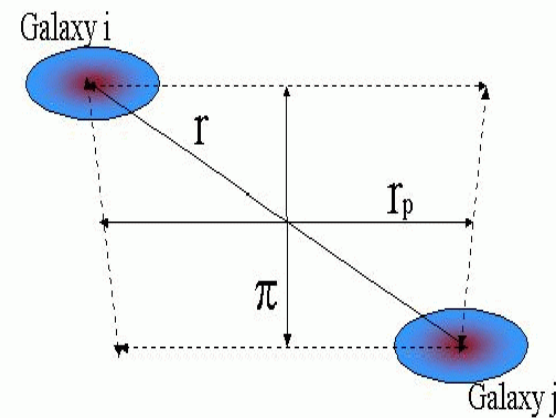
$$V = Hr + V_{\text{pec}}$$

Angular and 3D correlation functions

$$w(r_p) = 2 \int_{r_p}^{\infty} \xi(r) (r^2 - r_p^2)^{-1/2} dr$$

r_p : projected distance between pairs of galaxies,

Π : distance parallel to the line of sight



$$w(r_p) = \int_{-\delta\pi}^{+\delta\pi} \xi(r_p, \pi) d\pi$$



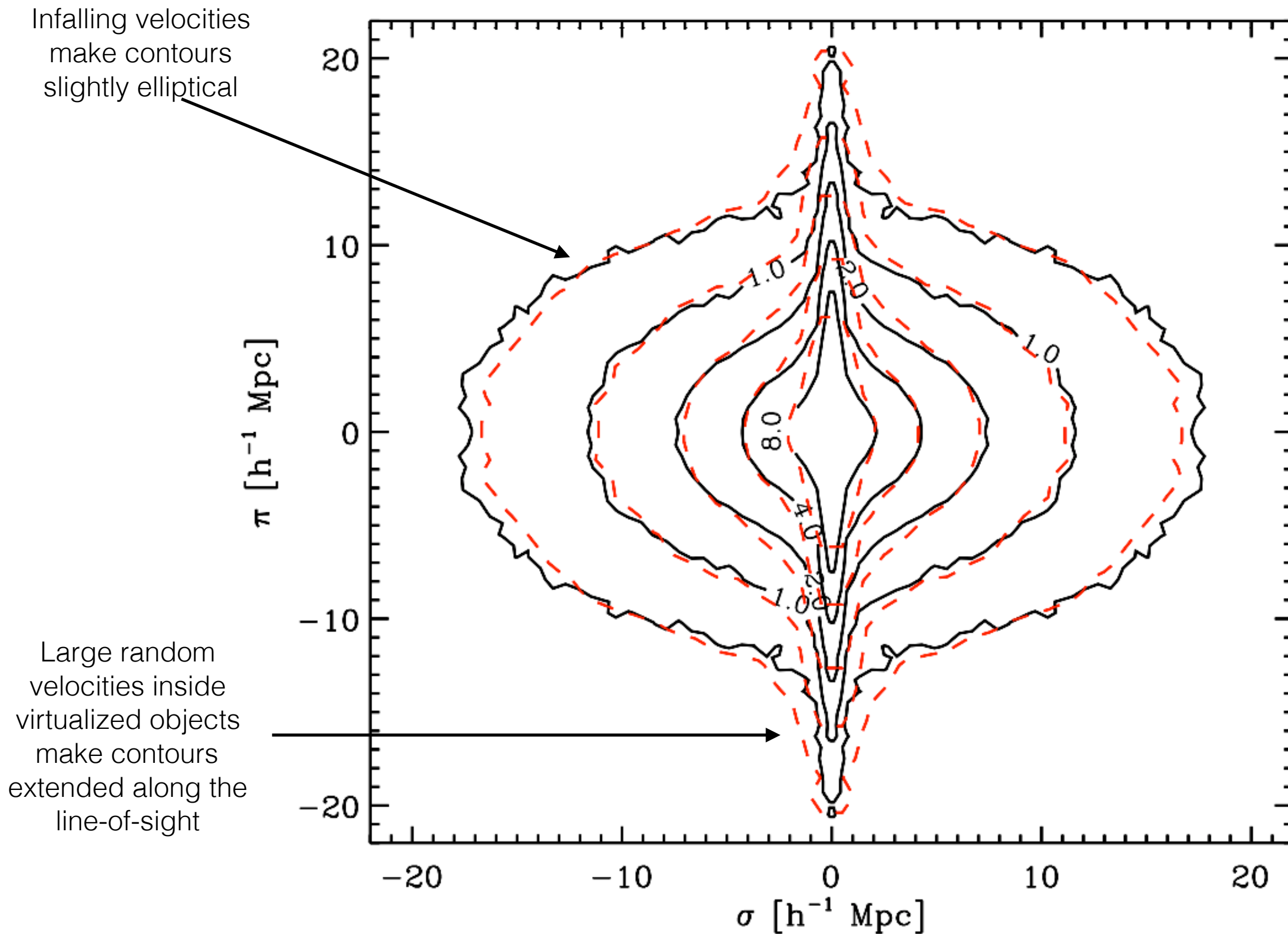
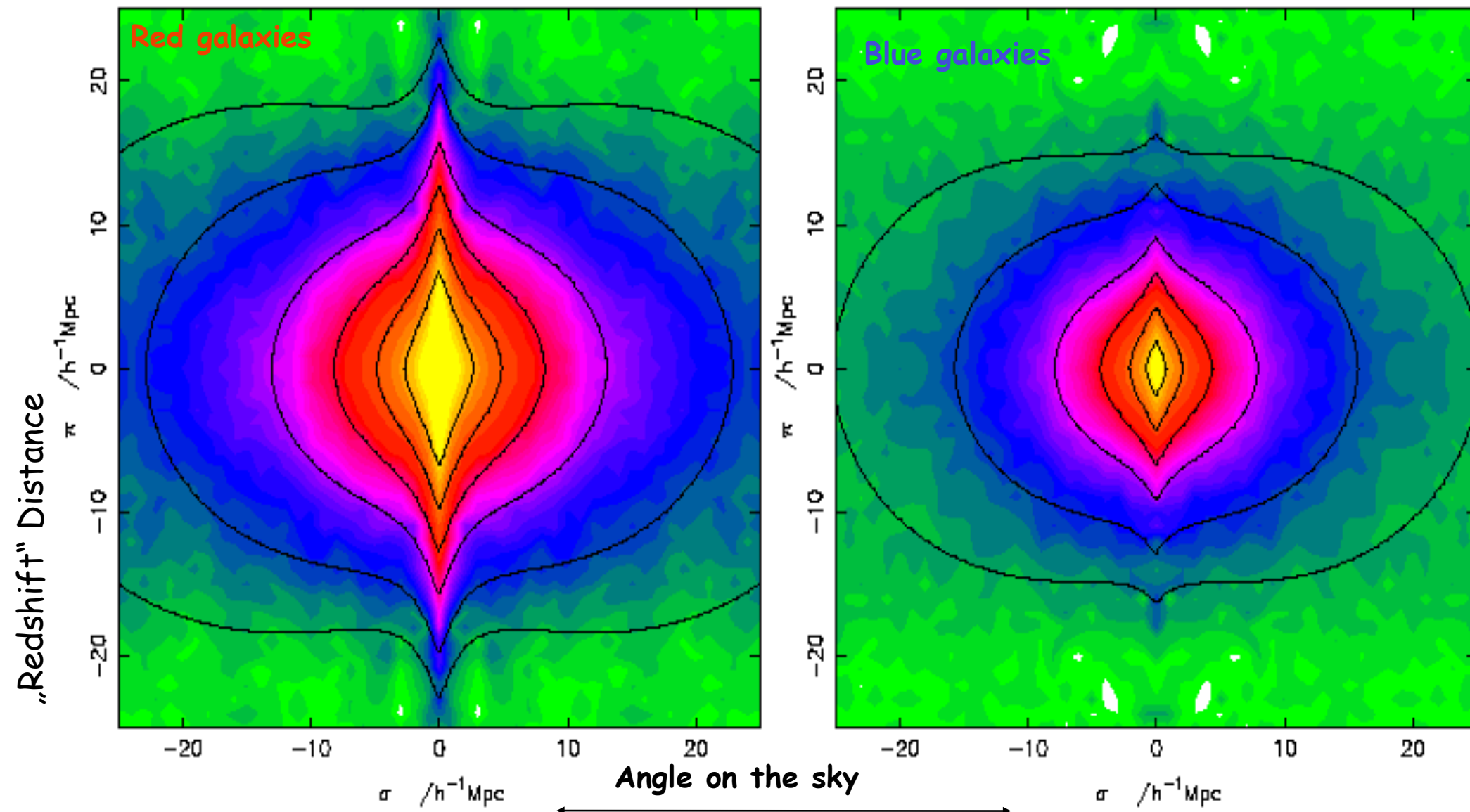


Figure 7. Contours of the two-dimensional correlation function $\xi(\sigma, \pi)$ estimated from the two-year BOSS-CMASS North galaxy sample (dashed line) at $0.4 < z < 0.7$ and for our MultiDark halo catalog constructed using the HAM technique at $z = 0.53$.

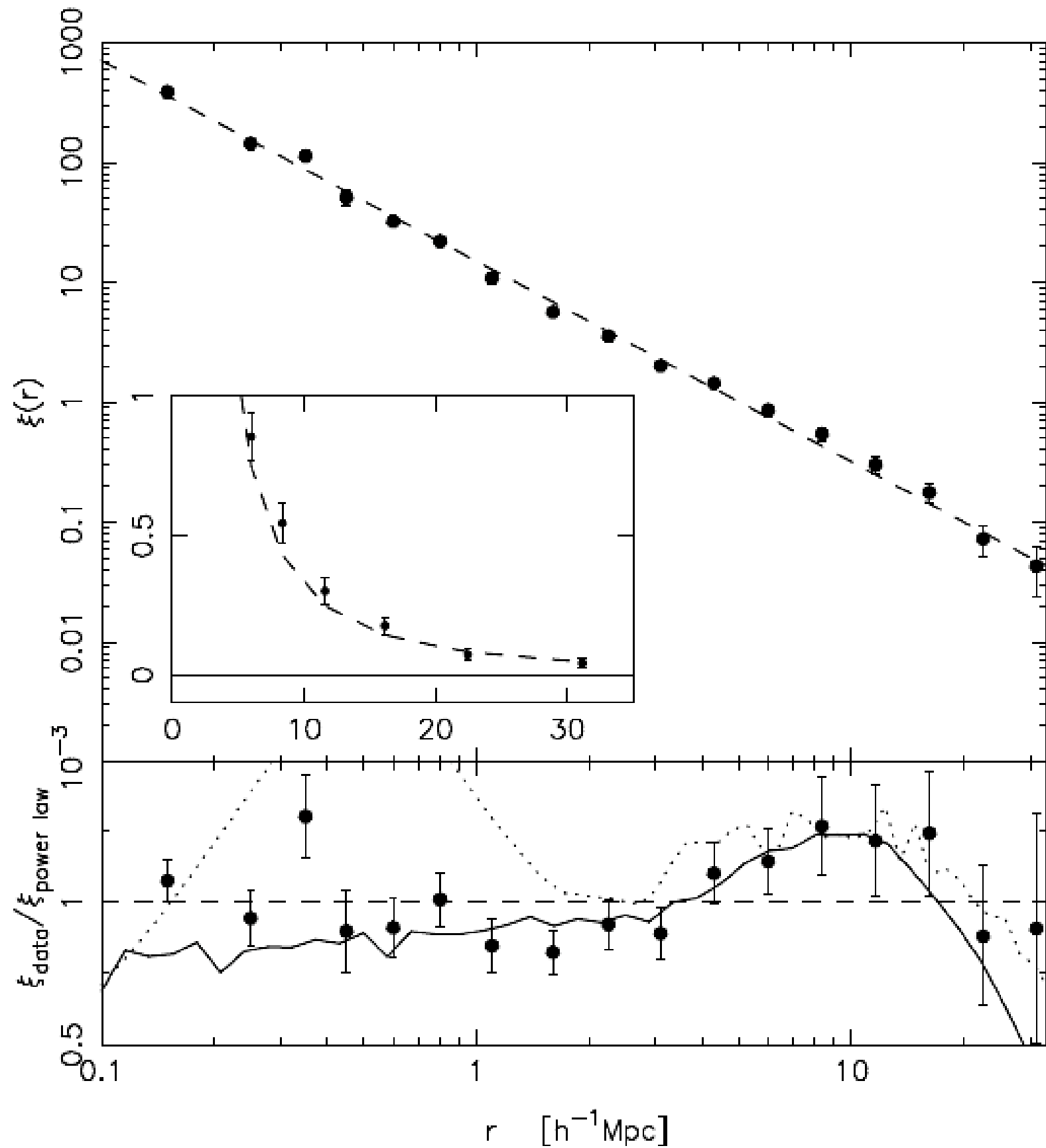
Redshift distortions: 'finger-of-god' effect on small scales



Galaxy Correlation Function

As measured
by the 2dF
redshift
survey

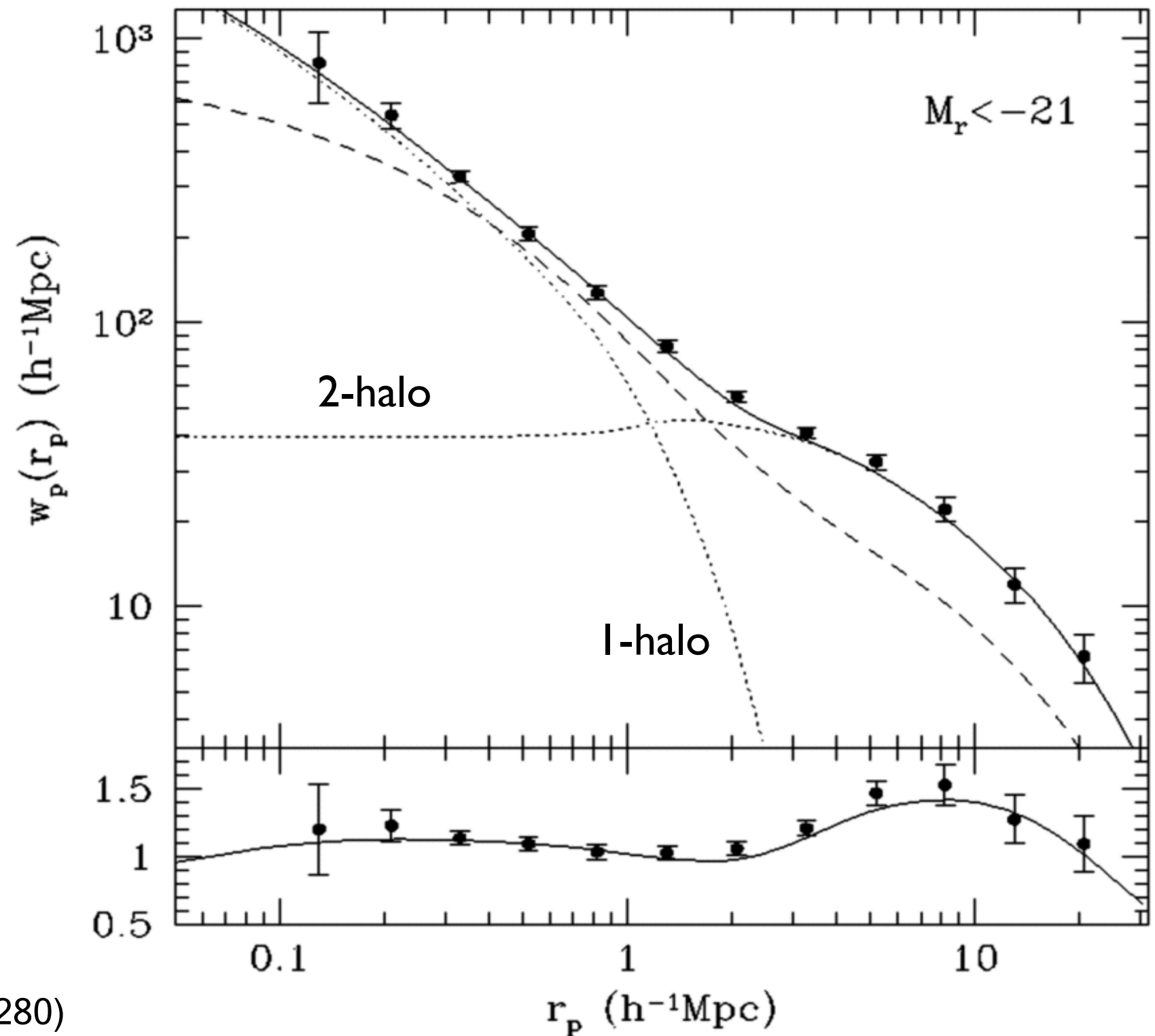
Deviations from
the power law:



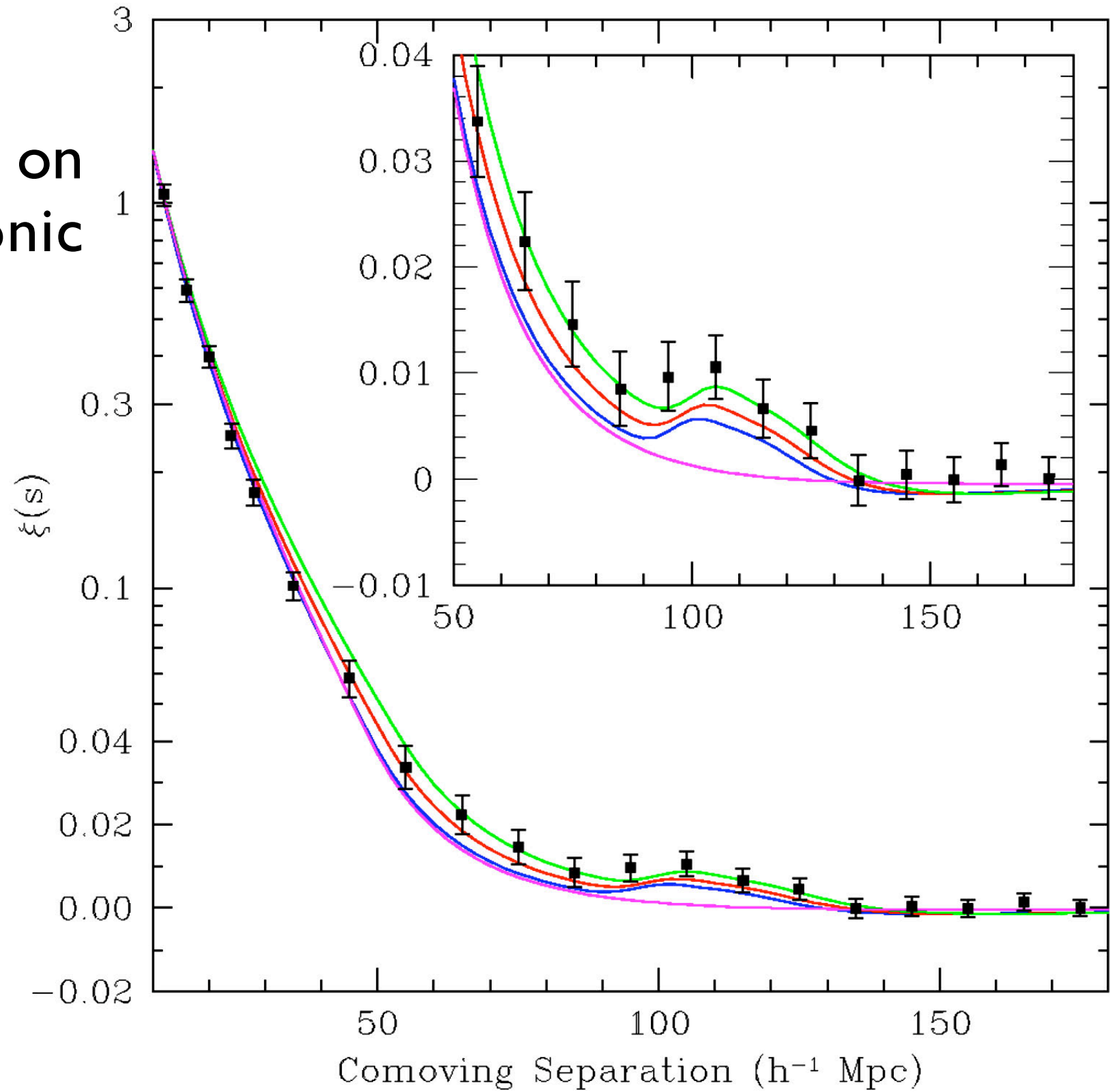
Angular correlation function: SDSS results

Two contributions:

- number-density profile of galaxies inside the same halo
- clustering of halos

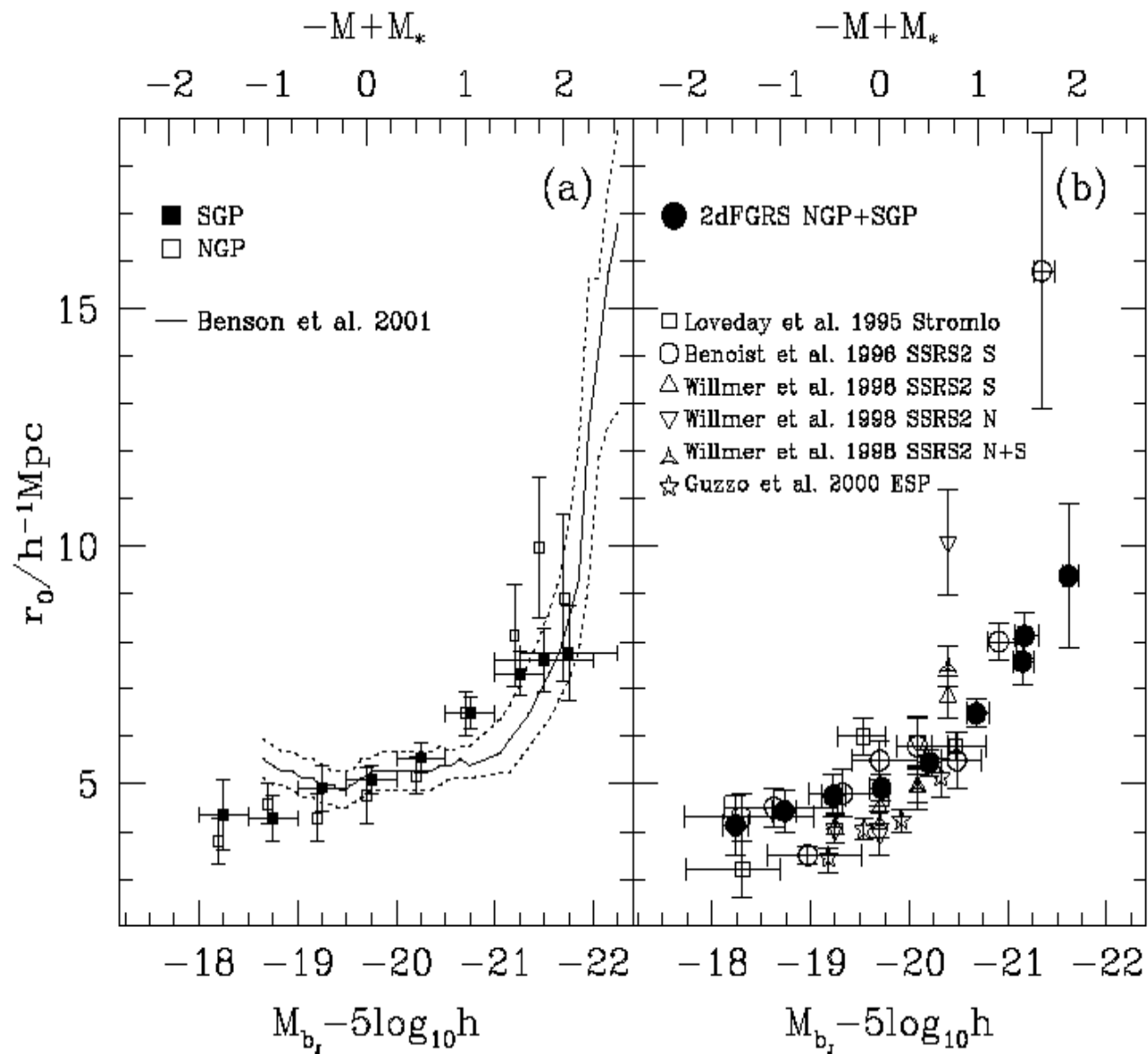


Correlation function on large scales: baryonic oscillations



SDSS (Eisenstein et al.)

Clustering of different galaxies



More luminous/massive galaxies are more strongly clustered

Clustering of different galaxies

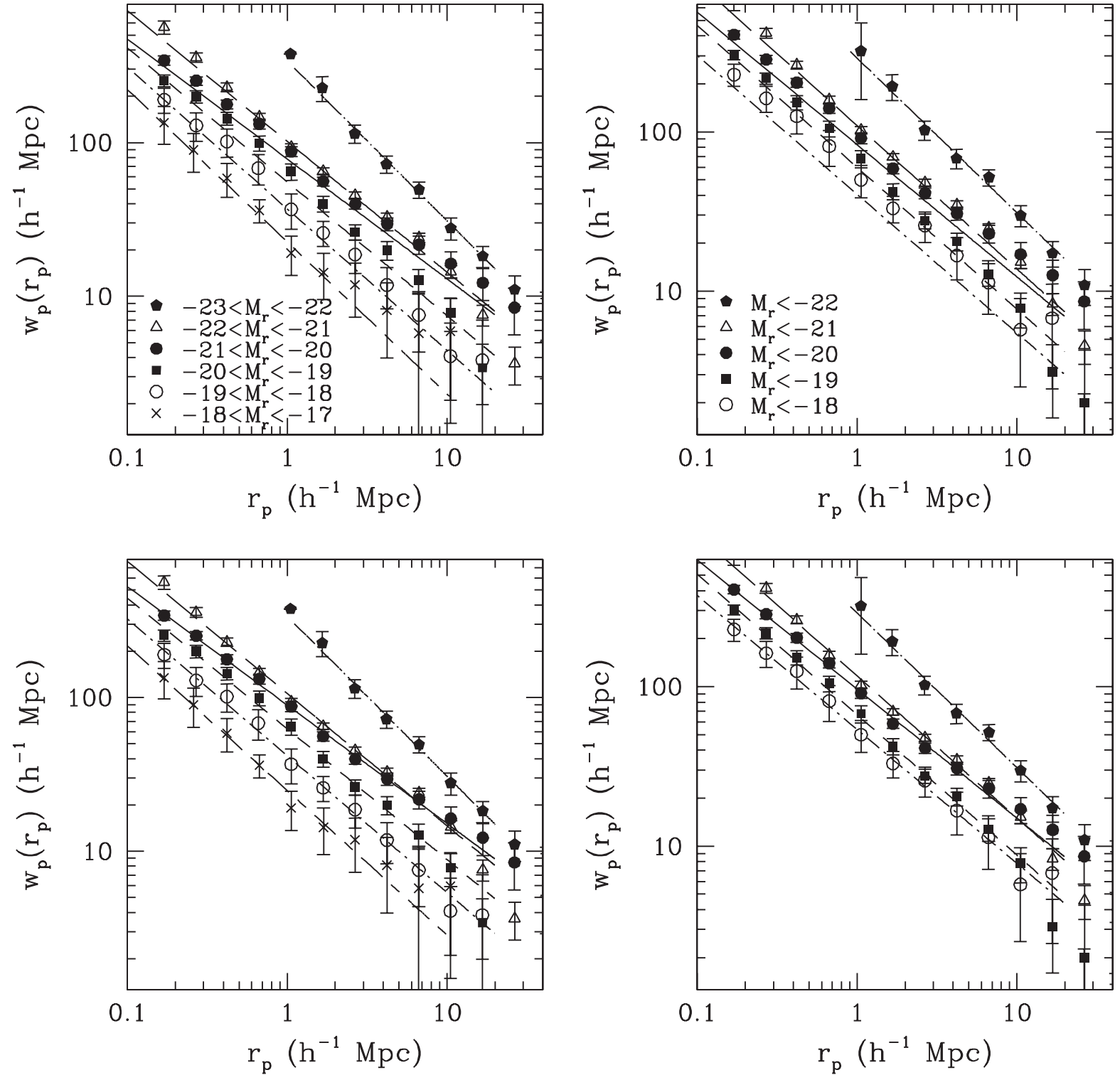
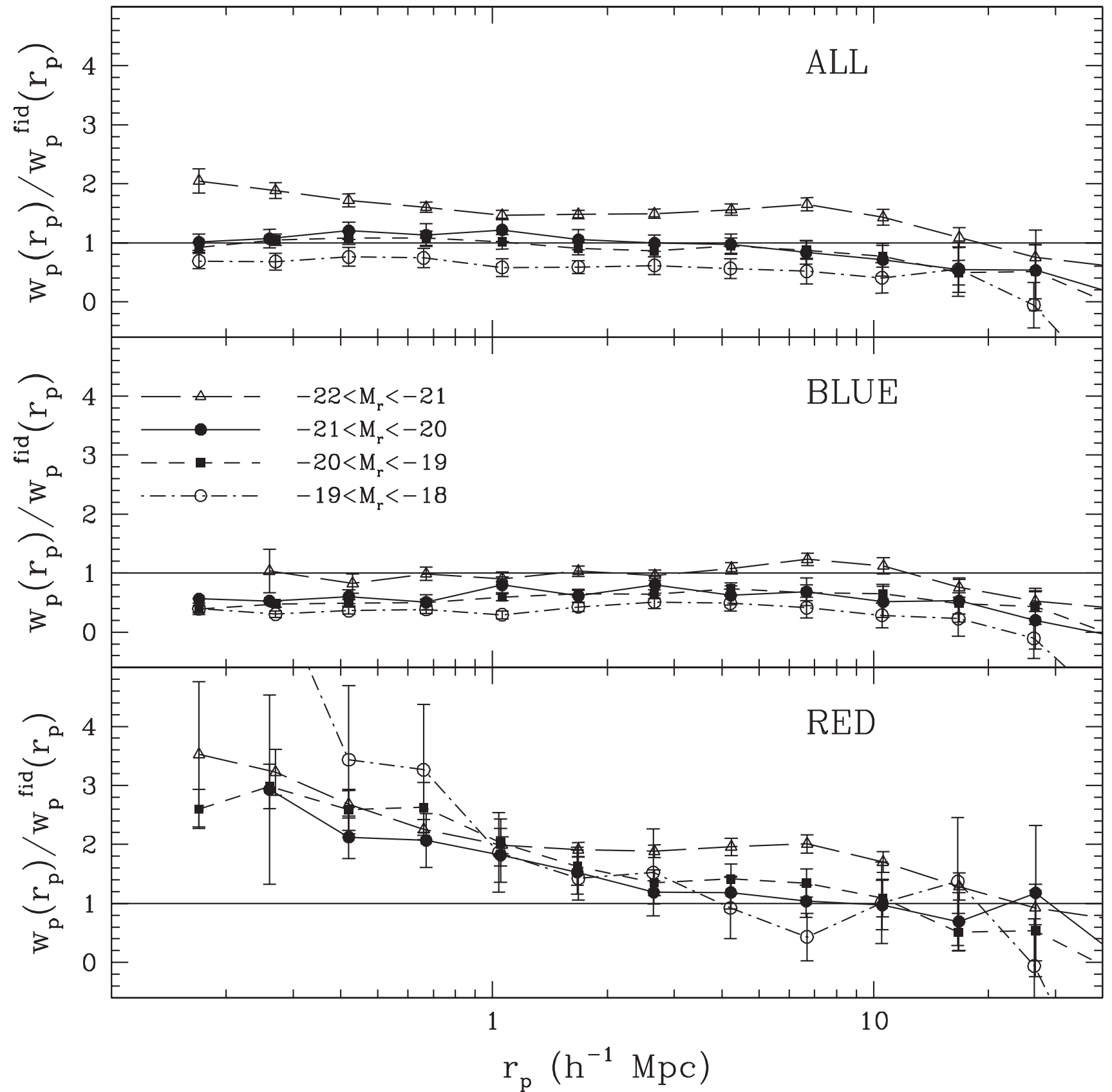


FIG. 8.—*Top left:* Projected galaxy correlation functions $w_p(r_p)$ for volume-limited samples with the indicated absolute magnitude and redshift ranges. Lines show power-law fits to each set of data points, using the full covariance matrix. *Top right:* Same as top left, but now the samples contain all galaxies brighter than the indicated absolute magnitude; i.e., they are defined by luminosity thresholds rather than luminosity ranges. *Bottom panels:* Same as the top panels, but now with power-law fits that use only the diagonal elements of the covariance matrix. [See the electronic edition of the Journal for a color version of this figure.]

Clustering: galaxy morphology



Bias $b^2 = W(r, \text{sample1})/W(r, \text{sample2})$

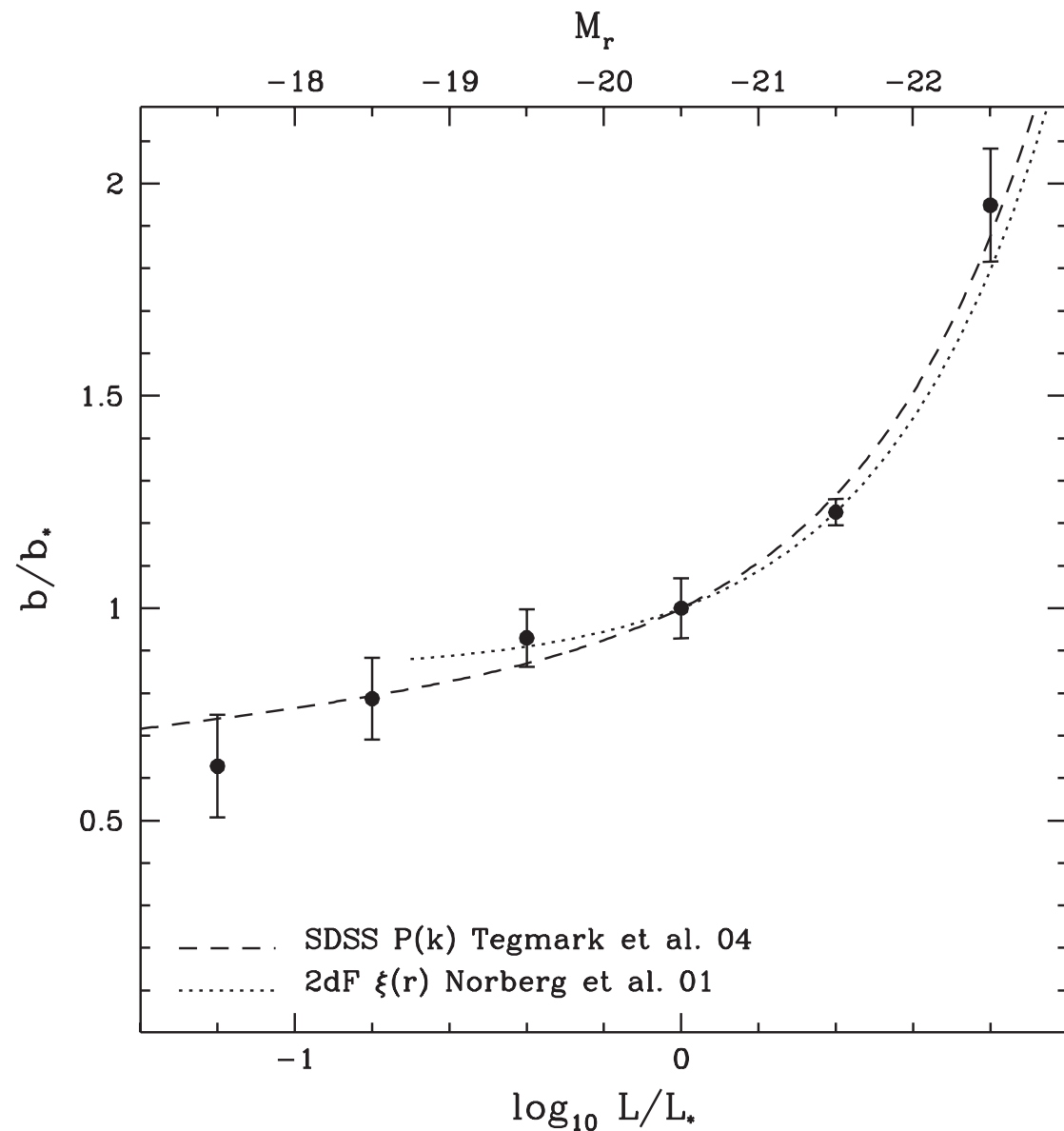
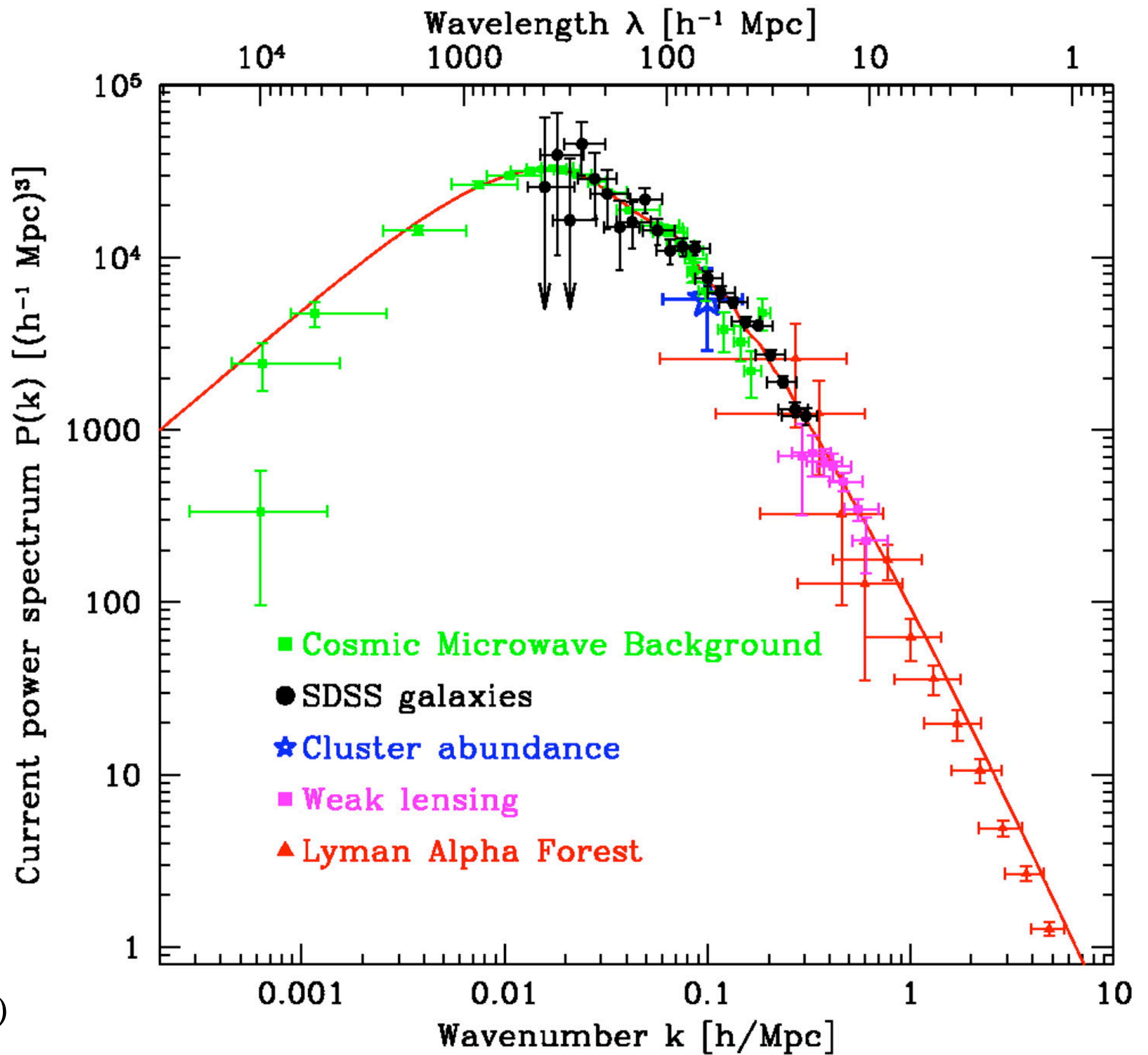


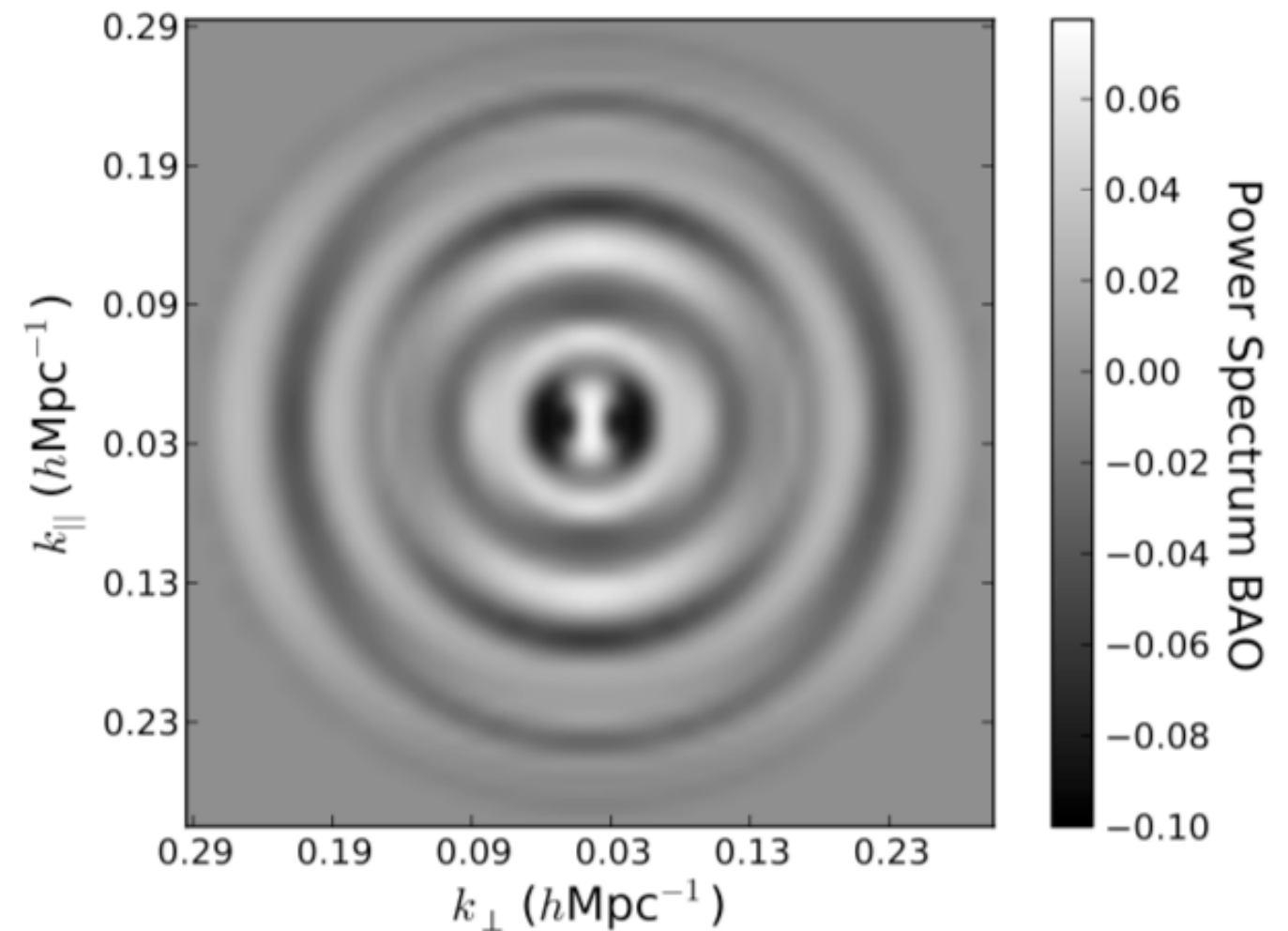
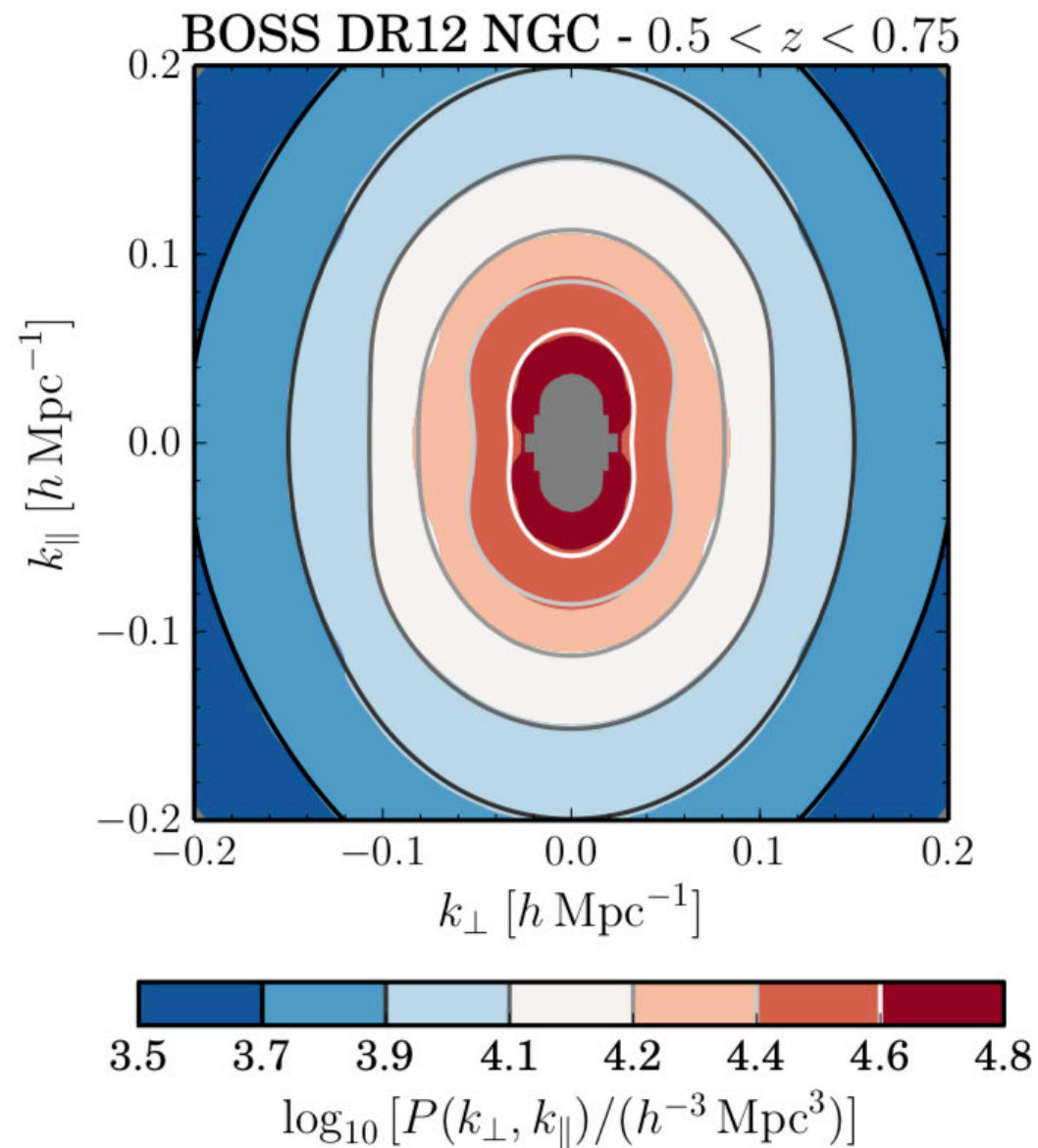
FIG. 11.—Relative bias factors for samples defined by luminosity ranges. Bias factors are defined by the relative amplitude of the $w_p(r_p)$ estimates at a fixed separation of $r_p = 2.7 h^{-1}$ Mpc and are normalized by the $-21 < M_r < -20$ sample ($L \approx L_*$). The dashed curve is a fit obtained from measurements of the SDSS power spectrum, $b/b_* = 0.85 + 0.15L/L_* - 0.04(M - M_*)$ (Tegmark et al. 2004a), and the dotted curve is a fit to similar $w_p(r_p)$ measurements in the 2dF survey, $b/b_* = 0.85 + 0.15L/L_*$ (Norberg et al. 2001).

The Observed Power Spectrum



(Tegmark et al.)

Baryonic acoustic oscillations: Power spectrum



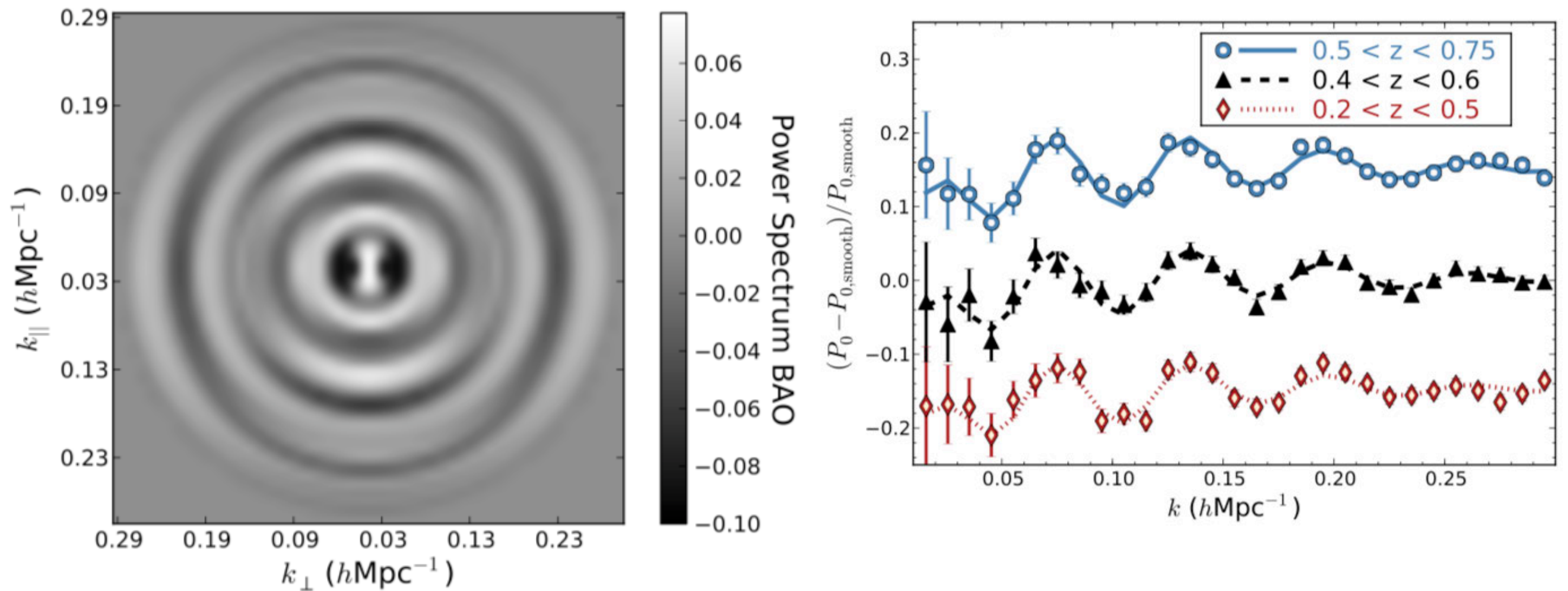
Power spectrum in redshift space.

Smooth background is subtracted

The clustering of galaxies in the completed SDSS-III Baryon Oscillation Spectroscopic Survey: cosmological analysis of the DR12 galaxy sample

Alam et al (BOSS) 2017

Baryonic acoustic oscillations: Power spectrum



Power spectrum in redshift space. Smooth background is subtracted

The clustering of galaxies in the completed SDSS-III Baryon Oscillation Spectroscopic Survey: cosmological analysis of the DR12 galaxy sample

Alam et al (BOSS) 2017

Baryonic acoustic oscillations: Power spectrum

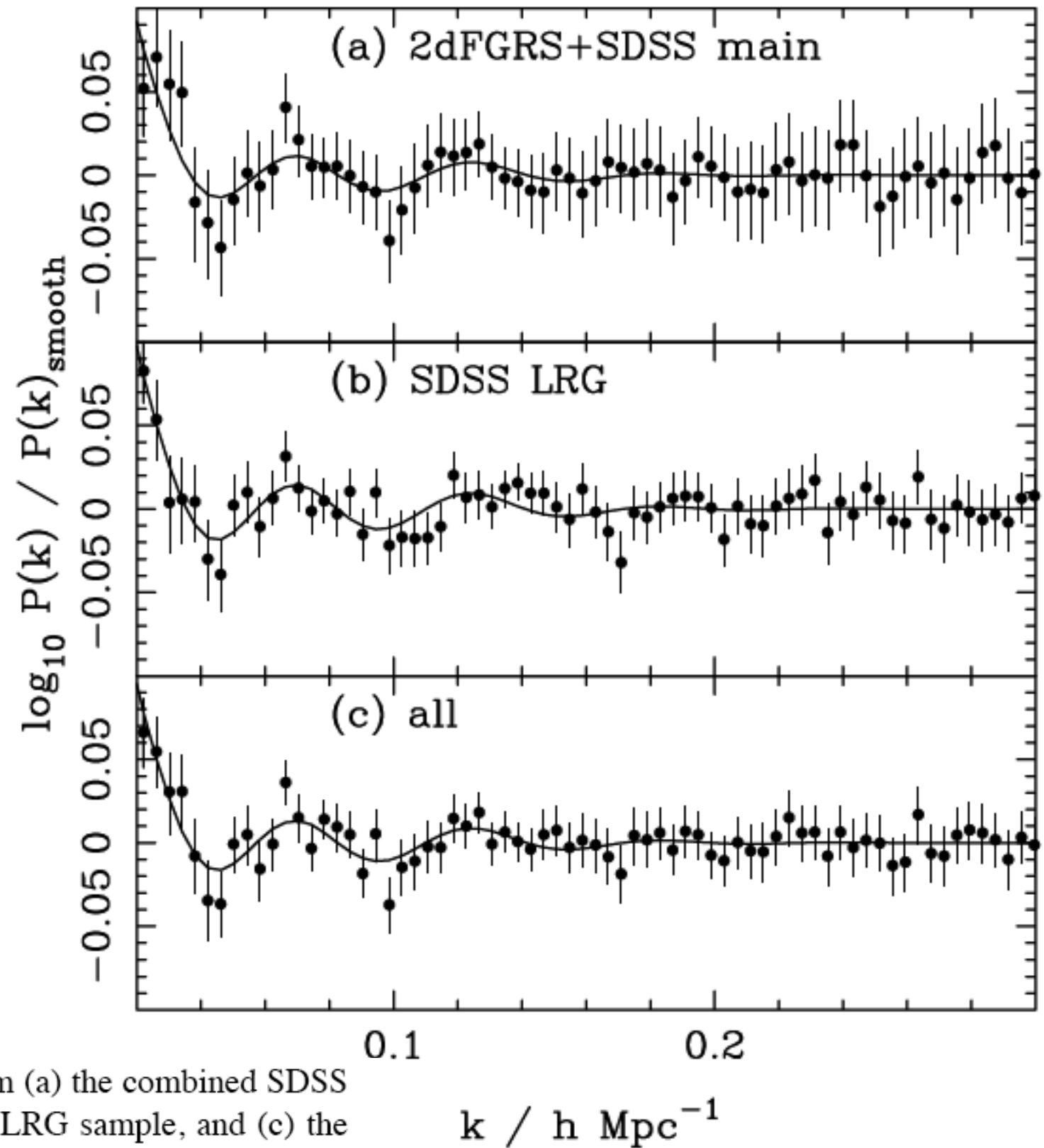


Figure 2. BAOs in power spectra calculated from (a) the combined SDSS and 2dFGRS main galaxies, (b) the SDSS DR5 LRG sample, and (c) the combination of these two samples (solid symbols with 1σ errors). The data are correlated and the errors are calculated from the diagonal terms in the covariance matrix. A standard Λ CDM distance–redshift relation was assumed to calculate the power spectra with $\Omega_m = 0.25$, $\Omega_\Lambda = 0.75$. The power spec-